The Plant Journal (2004) **40**, 752–771 doi: 10.1111/j.1365-313X.2004.02253.x

DNA array analyses of *Arabidopsis thaliana* lacking a vacuolar Na^+/H^+ antiporter: impact of AtNHX1 on gene expression

Jordan B. Sottosanto[1], Angie Gelli[2] and Eduardo Blumwald[1,*]
[1]*Department of Pomology, University of California, One Shields Ave, Davis, CA 95616, USA, and*
[2]*Department of Medical Pharmacology and Toxicology, University of California, One Shields Ave, Davis, CA 95616-8635, USA*

Received 20 July 2004; revised 23 August 2004; accepted 6 September 2004.
*For correspondence (fax +530 752 8502; e-mail eblumwald@ucdavis.edu).

Summary

AtNHX1, a vacuolar cation/proton antiporter of Arabidopsis, plays an important role in salt tolerance, ion homeostasis and development. We used the T-DNA insertional mutant of *AtNHX1* (*nhx1* plants) and *Affymetrix* ATH1 DNA arrays to assess differences in transcriptional profiles and further characterize the roles of a vacuolar cation/proton antiporter. Mature, soil-grown plants were used in this study to approximate typical physiological growing conditions. A comparison of plants grown in the absence of salt stress yielded many transcripts that were affected by the absence of the AtNHX1 vacuolar antiporter. Furthermore, changes in gene expression due to a non-lethal salt stress (100 mM NaCl) in the *nhx1* plants were significantly different from the changes seen in wild-type plants. The *nhx1* transcriptome was differentially affected when the plants were grown in the absence or presence of salt. In conclusion, in addition to the known role(s) of AtNHX1 on ion homeostasis, the vacuolar cation/proton antiporter plays a significant role in intracellular vesicular trafficking, protein targeting, and other cellular processes.

Keywords: AtNHX1, vacuolar Na^+/H^+ antiporter, knockout, DNA arrays, ion homeostasis, vesicular trafficking.

Introduction

Cellular ion homeostasis, the maintenance of optimal cellular ion concentrations, is of fundamental importance for growth and development in plants. Typically, plant cells maintain a low cytosolic Na^+ concentration that is attained by the operation of Na^+/H^+ antiporters located at both the plasma membrane (Shi *et al.*, 2000) and tonoplast (Apse *et al.*, 1999). Electrochemical H^+ gradients, generated by H^+-pumps at the plasma membrane (H^+-ATPase) and the tonoplast (H^+-ATPase, H^+-PP_iase), provide the energy used by the plasma membrane- and tonoplast-bound Na^+/H^+ antiporters to couple the passive movement of H^+ to the active movement of Na^+ out of the cell and into the vacuole, respectively (Blumwald, 1987). In *Arabidopsis thaliana*, the NHX family of vacuolar Na^+/H^+ antiporters comprises six members (AtNHX1–6). All vacuolar AtNHX proteins share some basic structural similarities, and AtNHX1–5 show functional Na^+/H^+ activity (Aharon *et al.*, 2003; Apse *et al.*, 1999; Yokoi *et al.*, 2002). Much interest in the occurrence and activity of vacuolar Na^+/H^+ antiporter activity in plants has been related to the study of salinity tolerance. Increased expression of *AtNHX1*, by transformation with *AtNHX1* driven by a strong constitutive promoter, has been shown to improve the tolerance to salinity of Arabidopsis (Apse *et al.*, 1999), *Brassica* (Zhang *et al.*, 2001), and tomato (Zhang and Blumwald, 2001). These results suggest that an increased capacity for vacuolar Na^+ sequestration is important for salinity tolerance. Other functions such as the regulation of vacuolar pH have also been suggested for NHX genes. The developing flower buds of morning glory change from purple to blue as the petals open. This process depends on the activity of an NHX1 homologue in *Ipomoema nil* (Yamaguchi *et al.*, 2001). However, it is not likely that this vacuolar pH regulation is dependent on sodium. The counter cation for proton extrusion from the vacuole is more likely to be potassium. AtNHX1 mediates the transport of K^+ as well as Na^+ in tonoplast vesicles isolated from tomato plants transformed with an overexpression construct of AtNHX1 (Zhang and Blumwald, 2001). AtNHX1 mediates both K^+/H^+ and Na^+/H^+ transport in liposomes reconstituted with purified AtNHX1 (Venema *et al.*, 2002).

Recently, a T-DNA insertional mutant of *AtNHX1* was characterized (Apse *et al.*, 2003). Vacuoles isolated from

leaves of the *nhx1* plants had much lower Na^+/H^+ and K^+/H^+ exchange activity, and the *nhx1* plants showed altered leaf development, with reduction in the frequency of large epidermal cells and a reduction in overall leaf area compared with wild-type plants. These results suggested that AtNHX1 is the dominant K^+ and Na^+/H^+ antiporter in leaf vacuoles in Arabidopsis and also that its contribution to ion homeostasis is important not only for salinity but also for developmental processes.

We conducted a transcriptome analyses using DNA microarrays of wild-type and *nhx1* plants grown in the absence and presence of salt to further characterize the role of AtNHX1. Transcriptome studies of salt stress have uncovered many aspects of altered transcriptional profiles in response to salt stress (Kawasaki *et al.*, 2001; Kreps *et al.*, 2002; Maathuis *et al.*, 2003; Seki *et al.*, 2002). In addition to the type of microarrays and the methods of analysis used, this work differs from the above-mentioned studies in several other aspects. Plants were grown in soil and exposed to sub-lethal levels of salinity for a relatively long period of time in order to characterize effects of altered ion homeostasis under typical growing conditions.

We used *nhx1* mutants to further characterize the role(s) of AtNHX1 in the Arabidopsis salt-stress response, and the effect(s) of altered ion homeostasis on the expression of other transcripts. Our results suggest that, in addition to its roles in ion homeostasis and salt tolerance, AtNHX1 influences other cellular processes.

Results and discussion

Data set filtering and analyses

This report focuses on three different comparisons of global transcription levels using *Affymetrix*® *GeneChip*® microarrays (Affymetrix, Santa Clara, CA, USA). The first comparison measures differences of transcription between *nhx1*, an *Arabidopsis thaliana* plant line with a T-DNA 'knockout' insertional mutation of the vacuolar Na^+/H^+ antiporter *AtNHX1*, and wild-type Arabidopsis grown under 'control' conditions (without salt stress). The second and third comparisons examine the transcriptional changes resulting from 2 weeks extended exposure to 100 mM NaCl treatment of both *nhx1* and wild-type plants, with control treatment profiles for the respective plant lines providing a baseline. To determine meaningful differences between samples, two different statistical cut-offs were used: (i) a cross-wise comparison ratio analysis method to establish transcripts that had at least a 50% change, and (ii) a Student's *t*-test comparison to verify that the differences were consistent (see Experimental procedures). Among the 13 144 transcripts with reliable expression data, 3 780 genes met at least one of these criteria in at least one of the three comparisons. Data for these transcripts can be found online at http://blumwald.ucdavis.edu/microarrays.shtml

Using both statistical methods, the expression levels of 83 genes were significantly increased in the *nhx1* knockout line compared with the wild type, and the expression levels of 98 genes were significantly decreased under control growing conditions. After 2 weeks of growth in the presence of 100 mM NaCl, the wild-type line displayed a significantly increased expression of 133 transcripts, and a significantly decreased expression of 252 genes, whereas the *nhx1* knockout line had 128 and 219 genes with expression that was significantly increased or decreased, respectively, when compared with growth in the absence of salt treatment. Tables with the comparison data for the significantly changed transcripts can be viewed with the online version of this article (Tables S1–S4).

The above-mentioned genes were classified according to a number of functional categories, based on a modification of the functional annotation suggested by the MIPS MATDB web database (TIGR and TAIR websites were also consulted, particularly in those cases of unclear gene function). For all transcripts, functional classification was assigned based on the most likely role of the predicted gene product (see Experimental procedures).

The transcripts reported as significant in this report are ones with primarily mid-level expression. By eliminating transcripts that were not considered present, based on perfect match/mismatch probe comparisons (see Experimental procedures), transcripts displaying low expression levels and inherent unreliability were removed from the analysis. On the other end of expression levels, because only transcripts with at least a 50% change were analyzed, many of the transcripts with higher levels of expression were not represented, although there may be a consistent pattern of change between experimental conditions. Further significance was established using the Student's *t*-test using a cut-off of $P < 0.05$. Many transcripts, at all ranges of expression, met this second criterion without showing a minimum change of 50%. The experimental conditions used in this study (2 weeks of growth in the presence of non-lethal NaCl concentrations, growth in soil, 1-month-old seedlings, heterogeneous tissue sampling) could allow for the identification of minimal, albeit meaningful, changes of expression. Nevertheless, these minimal changes are out of the scope of this report.

The microarray analyses were partially verified (18 transcripts) using a quantitative real-time polymerase chain reaction (q-RTPCR) approach (see Experimental procedures) (Figure 1). Altogether, the two methods provided correlating data. The trends of both increased and decreased expression for the comparisons were similar. While there were several examples of q-RTPCR comparisons with $\log_2$ ratios smaller (and some larger) than what was obtained with microarrays, both methods agreed. The q-RTPCR data had larger

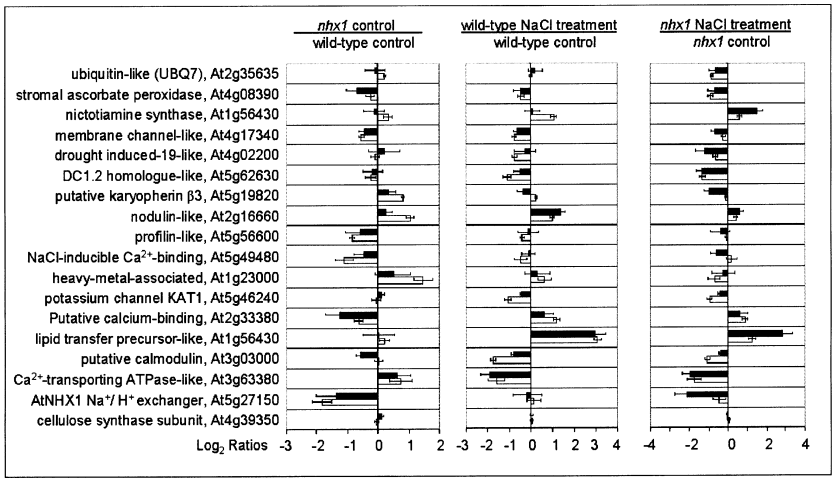

Figure 1. Comparison of relative transcript abundance measured by q-RT-PCR versus DNA microarrays methods. Gene names and accession numbers are indicated.
White bars: microarrays; black bars: qRT-PCR. Values are mean ± SE ($n > 3$).

standard errors because of increased sensitivity (Klien, 2002) and fewer experimental data points (a cross-wise comparison was not performed with q-RTPCR as the data and comparisons of each data replicate were analyzed separately).

While it is difficult to obtain consistent results from biological replicates using microarray analysis (Lee *et al.*, 2000; Pan *et al.*, 2002), especially with a heterogeneous tissue sample (i.e. whole leaves) as in this study, the simple methods used here established transcripts that were significantly altered in their expression levels. The statistical confidence level of our results suggests that more than 95% of the results reported are the result of real biological changes of transcription. Not all of the transcripts that met the full criteria set by this report are discussed. Although each significant change of transcription may reflect the key role of a particular gene, this report focuses on those transcripts that, based on a current understanding of biological processes, would appear most meaningful to the role of AtNHX1 and/or the response of Arabidopsis to salt stress.

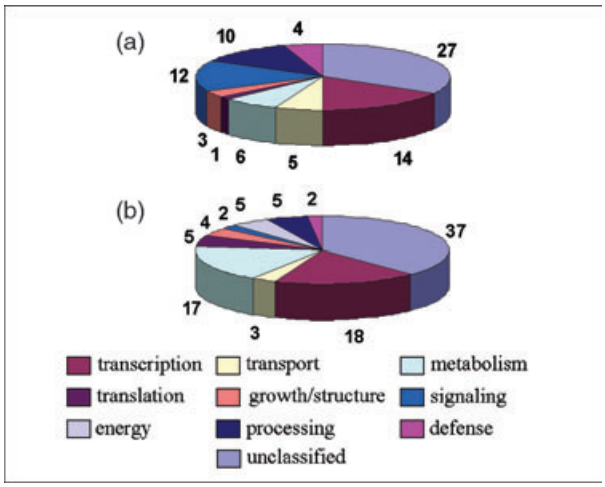

Figure 2. Relative distribution of altered transcripts in the *nhx1* knockout line.
The pie charts represent (a) 83 transcripts displaying increased expression and (b) 98 transcripts displaying decreased expression in the *nhx1* knockout plants compared with the wild-type plants grown under control conditions. Criteria used to assign function are described in Experimental procedures.

Transcriptional differences due to the absence of a functional AtNHX1

T-DNA insertional mutants of *AtNHX1* (*nhx1*) displayed altered ion homeostasis, smaller leaves and epidermal cells, and other phenotypical characteristics (Apse *et al.*, 2003). In order to further characterize the role(s) of AtNHX1 in plant development and other key physiological processes, the transcriptional profiles of wild-type plants and the insertional mutants were compared by DNA microarray analyses.

Increased expression. Figure 2(a) (also Table S2) illustrates the functional categories represented by those 83 genes with increased expression in the *nhx1* line. The only functional group not represented among these genes was energy-related genes, suggesting that in the *nhx1* plants there was not a surplus of energy production and/or utilization. Moreover, only one translation-associated transcript, with an undefined role, appeared to be induced suggesting that there was no significant increase in overall protein synthesis in the knockout plants.

Fourteen genes encoding transcription factors and other DNA-binding proteins displayed increased transcription in the *nhx1* line (Table 1). Most of these (11 genes) have domains involved in the regulation of specific gene expression and developmental regulation. One transcript that stands out with regard to the possible influence of *AtNHX1* on developmental processes is a CCCH-type [PF00642] zinc-finger (At1g19860) that has similarities to the homeobox LUMINIDEPENDENS protein At4g02560, known to regulate flower timing and other cell proliferation events (Aukerman

Table 1 Transcripts of interest displaying increased expression in the *nhx*1 line[a]

Functional classification[b]	Accession	Description	Mean ± SE[c]	*P*[d]
Transcription	At1g33470	RNA binding	2.49 ± 0.55	0.01
	At1g72830	CCAAT-binding factor B subunit homolog	2.13 ± 0.43	0.04
	At5g62000	Auxin response factor-like	1.48 ± 0.22	0.02
	At5g67580	Telomere repeat-binding factor 2, myb family (TRB2)	1.22 ± 0.10	0.00
	At1g77300	SET domain	1.20 ± 0.27	0.03
	At1g19860	CCCH-type zinc finger	1.12 ± 0.13	0.00
	At2g19120	Putative DNA2-NAM7 helicase family	1.09 ± 0.20	0.00
	At5g02860	crp1	1.01 ± 0.20	0.03
	At1g21200	Putative transcription factor	1.00 ± 0.20	0.04
	At2g31640	Putative PHD-type zinc finger	1.00 ± 0.08	0.00
	At2g16090	Zinc finger-related	0.93 ± 0.12	0.00
	At1g16190	UV-sensitive rad23	0.92 ± 0.14	0.02
	At3g15030	Similar to TCP3	0.85 ± 0.12	0.01
	At3g60320	bZIP	0.71 ± 0.05	0.00
Transport	At4g16480	Membrane sugar transporter-like	1.57 ± 0.31	0.02
	At1g23000	Heavy metal binding	1.49 ± 0.20	0.01
	At3g60160	ABC transporter (AtMRP9)	1.28 ± 0.28	0.04
	At5g09400	Potassium transport (AtHAK7)	1.13 ± 0.15	0.01
	At2g16660	Nodulin-like protein	1.06 ± 0.14	0.01
Signaling	At5g49780	Receptor protein kinase-like	1.62 ± 0.27	0.00
	At1g11130	Leucine-rich repeat transmembrane protein kinase	1.30 ± 0.22	0.02
	At1g66880	Protein kinase	1.19 ± 0.28	0.03
	At1g53440	Receptor-like serine/threonine kinase	1.13 ± 0.12	0.00
	At3g50590	G protein beta WD-40 repeats	1.10 ± 0.25	0.03
	At5g23350	Similarity to ABA-responsive protein	1.08 ± 0.20	0.04
	At5g50970	G protein beta WD-40 repeats	1.05 ± 0.14	0.01
	At5g41180	Receptor kinase-like	1.04 ± 0.13	0.01
	At2g45670	Calcineurin B subunit-related	1.02 ± 0.15	0.01
	At2g30520	Signal transducer of phototropic response (RPT2)	1.01 ± 0.15	0.02
	At5g02760	Protein phosphatase 2C homolog	1.00 ± 0.20	0.03
	At5g03040	Calmodulin-binding motif	0.94 ± 0.08	0.00
Processing	At2g36130	Cyclophilin-like	1.55 ± 0.23	0.01
	At3g19730	Dynamin-like, similar to phragmoplastin	1.46 ± 0.34	0.02
	At2g43160	Putative clathrin-binding protein (epsin)	1.32 ± 0.24	0.02
	At3g17970	Chloroplast TOC subunit, amidase-like	1.28 ± 0.19	0.00
	At4g27640	Putative Ran_GTP binding protein 5	1.05 ± 0.20	0.05
	At1g55350	n-calpain-1 large subunit	1.01 ± 0.14	0.01
	At2g25490	F-box protein family (AtFBL6)	0.96 ± 0.16	0.02
	At2g31900	Putative unconventional myosin	0.94 ± 0.16	0.03
	At3g55150	Leucine zipper-containing	0.87 ± 0.10	0.00
	At5g19820	Karyopherin beta 3 like, PBS lyase HEAT-like repeat	0.82 ± 0.06	0.00
Growth/structure	At1g02200	Receptor-like protein glossy1 (CER1)	1.44 ± 0.30	0.01
	At3g23670	Kinesin-like	1.33 ± 0.16	0.00
	At1g29400	RNA-binding protein MEI2	1.01 ± 0.12	0.00
	At2g43150	Putative extension	0.95 ± 0.14	0.01

[a]The complete table of the 83 transcripts with increased expression in the *nhx1* line can be found in Table S1.
[b]Functional characterization is described in Experimental procedures.
[c]Mean numbers represent the $\log_2$ transformed ratios (experimental/baseline ± SE) generated by cross-comparing the replicate data sets of the *nhx1* line with the wild-type line.
[d]Student's *t*-test *P*-values for data comparison.

et al., 1999). This transcript may be contributing to the earlier bolting and flowering phenotype of the *nhx1* line when compared with wild type (Apse *et al.*, 2003). The other three genes encoding DNA-binding proteins are associated with more global aspects of gene transcription, including a telomere-binding protein (TRB2/At5g67580) that may be working in conjunction with a putative DNA repair protein (rad23/At1g16190), to possibly address oxidative damage and abnormal cell cycle conditions in the *nhx1* line (Narayan *et al.*, 2001).

Five genes encoding transporters were significantly upregulated in the *nhx1* line. These genes encode a heavy metal-binding protein (At1g23000) similar to a copper homeostasis factor, a potassium transporter (AtKT7/HAK7/KUP7/At5g09400); a nodulin-like protein (At2g16660) with an unassigned transport role, a sugar transporter (At4g16480); and an uncharacterized ABC-transporter (AtMRP9/At3g60160). Each of these proteins may be playing an important compensatory role in the knockout line, although that remains to be established by other methods. AtKT7/HAK7/KUP7 complements *Escherichia coli* mutants deficient in K^+ uptake, confirming its role in K^+ transport (Ahn *et al.*, 2004). The mechanisms by which this protein contributes to K^+ uptake and ion homeostasis are not fully understood and it has been postulated that some of the members of the gene family are involved in vacuolar transport (Senn *et al.*, 2001). In *Mesembryanthemum crystallinum* the expression of these genes was enhanced by K^+ starvation (Su *et al.*, 2002) further suggesting their role in K^+ homeostasis. AtNHX1 mediates the transport of Na^+ and K^+ into the vacuoles (Apse *et al.*, 1999; Zhang and Blumwald, 2001). We hypothesize that the absence of functional AtNHX1 affects the movement of K^+ into the vacuole (Apse *et al.*, 2003), perturbing K^+ homeostasis and promoting the induction of AtKT/HAK/KUP7.

Also of interest are the 10 transcripts encoding proteins that appear to participate in the processing, modification, and targeting of other proteins to cellular components that also showed increased expression in the *nhx1* line. In particular, a putative clathrin-binding protein with an ENTH [PF01417] domain (At2g43160); a protein (At3g55150) that is similar to a yeast exocytosis gene - EXO70 [PF03081]; a protein (At3g17960) with strong similarity to a TOC (Toc64) subunit in pea; a PBS lyase HEAT-like repeat [PF03130] containing protein (At5g19820) likely involved in protein nucleus import and similar to karyopherin β3 from humans; an importin β-2 subunit family protein (At4g27640) also with a HEAT-domain and likely also involved in protein nucleus import; a dynamin-like protein similar to phragmoplastin (At3g19730); and an unconventional myosin protein (At2g31900). The presence of the transcripts related to vesicular trafficking is notable because Nhx1p, the yeast ortholog of AtNHX1, plays an important role in protein trafficking in yeast (Ali *et al.*, 2004; Bowers *et al.*, 2000). The change in expression of genes encoding proteins involved in cytosolic protein trafficking (dynamin and clathrin-binding proteins) and trafficking to the nucleus and organelles (small GTPase, TOC, karyopherin) suggests altered endosomal protein trafficking in the *nhx1* knockout line.

Decreased expression. Of the 98 transcripts that had significantly lower expression levels in the knockout line (Figure 2b, Table 2, Table S3), four were translation-associated (ribosomal) genes and seven were energy-associated, suggesting compromised synthetic and catabolic activities in the *nhx1* plants. This was also reflected in the 17 metabolism-associated transcripts that were similarly diminished.

Although it is difficult to elucidate the significance of the downregulation of 18 genes encoding different transcription factors and DNA-binding proteins, they may be key to the developmental and phenotypical characteristics of the *nhx1* line. Of these transcription factors and DNA-binding proteins with diminished expression levels, seven appear to interact with transcriptional processes in a non-specific manner and may be part of more general transcription or replication processes, including an RNA polymerase subunit (At5g24120), a nuclear cap-binding protein (CBP20/At5g44200), a chromosome assembly homolog (At3g52900) and genes encoding histone components (At2g38810, At2g2870). These diminished transcripts are likely involved in cell division and growth, and the decreased expression may be contributing to the smaller cell size and other developmental abnormalities of the *nhx1* line (Apse *et al.*, 2003). The other 11 diminished transcripts include genes with putative zinc finger, homeobox, or other domains associated with more direct regulation of gene expression. Interestingly, in this category is a NAM family [PF02365] transcript (RD26/At4g27410), previously shown to be drought-inducible (Taji *et al.*, 1999), suggesting that this transcript differentially responds to conditions of altered homeostasis.

In addition to *AtNHX1*, two other genes encoding proteins involved in ion homeostasis also showed diminished expression: a copper-binding/homeostasis factor family protein (GMFP7-like/At3g48970) and a metallothionein-like protein (MT1C/At1g07610) that also appears to bind copper. Neither of these transcripts appears to encode transmembrane transporters, although they might reflect a possible role of metal-binding proteins for adaptation to conditions of altered ion homeostasis. Copper ions are essential cofactors for enzymes implicated in the oxidative stress response and other important cellular processes (Rees and Thiele, 2004), and a link between copper and vacuolar processing has been suggested (Szczypka *et al.*, 1997). While a direct link between copper-processing/signaling and the AtNHX1 antiporter has not been established, these results (and the results shown later in this report) suggest a significant relationship between the two cellular components.

Five transcripts associated with protein processing and vesicular trafficking were also downregulated in *nhx1* plants. Among these, genes encoding a clathrin coat-like protein (At3g50860), a DnaJ [PF00226] protein (At3g14200) and a heat-shock protein (At1g53540). Also reduced in expression were a UBX (ubiquitin binding) domain-containing [PF00789] protein (At4g10790) and a putative Golgi *N*-acetylglucosaminyl transferase [PF05060] (At2g05320) that may be involved in protein degradation and modification, respectively. The decreased expression of genes encoding

Table 2 Transcripts of interest displaying decreased expression in the *nhx1* line[a]

Functional classification[b]	Accession	Description	Mean ± SE[c]	*P*[d]
Transcription	At1g22590	Putative DNA-binding protein	−1.79 ± 0.16	0.01
	At5g24120	Sigma-like factor	−1.56 ± 0.28	0.01
	At4g27410	Putative (NAM-like)	−1.50 ± 0.15	0.01
	At5g45700	NIF//NLI interacting factor	−1.43 ± 0.32	0.04
	At5g39550	Zinc finger-like	−1.35 ± 0.32	0.05
	At1g16640	Transcriptional factor B3 family	−1.30 ± 0.19	0.01
	At2g28740	Histone H4	−1.14 ± 0.22	0.04
	At2g38810	Histone H2A	−1.11 ± 0.24	0.03
	At2g36480	Zinc finger (C2H2-type) family protein	−1.09 ± 0.20	0.02
	At3g52900	Chromosome assembly protein homolog	−1.03 ± 0.17	0.03
	At2g45530	Zinc finger	−0.99 ± 0.18	0.02
	At2g19380	RNA recognition	−0.98 ± 0.17	0.02
	At4g30330	Small nuclear ribonucleoprotein homolog E	−0.97 ± 0.18	0.03
	At3g02340	C3HC4 type RING zinc-finger	−0.96 ± 0.17	0.03
	At5g44200	Nuclear cap-binding (CBP20)	−0.86 ± 0.13	0.01
	At5g64950	mTERF domain	−0.85 ± 0.08	0.00
	At4g15090	FAR1 family transposable element	−0.84 ± 0.12	0.01
	At5g42780	Zinc finger homeobox	−0.82 ± 0.09	0.00
Transport	At5g27150	AtNHX1 Na+/H+ exchanger	−1.83 ± 0.27	0.00
	At1g07610	Metallothionein-like	−1.06 ± 0.20	0.03
	At3g48970	Putative GMFP7 isoprenylated protein	−1.04 ± 0.22	0.03
Signaling	At2g36570	Putative receptor-like protein kinase	−1.27 ± 0.21	0.01
	At5g49480	NaCl-inducible calmodulin-like	−1.09 ± 0.24	0.01
Processing	At5g37670	Low-molecular-weight heat shock	−1.73 ± 0.25	0.04
	At3g14200	dnaJ	−1.56 ± 0.25	0.01
	At3g50860	Putative clathrin coat assembly	−1.20 ± 0.29	0.03
	At4g10790	UBX domain containing	−0.98 ± 0.10	0.00
	At2g05320	*N*-acetylglucosaminyl transferase-like	−0.95 ± 0.14	0.01
Growth/structure	At4g13210	Pectate lyase	−1.36 ± 0.24	0.03
	At4g30450	Glycine-rich cell wall protein	−1.02 ± 0.12	0.00
	At4g08160	Putative xylan endohydrolase	−0.84 ± 0.12	0.01
	At5g56600	Profilin-like	−0.84 ± 0.08	0.00

[a]The complete table of the 98 transcripts with increased expression in the *nhx1* line can be found in Table S2.
[b]Functional characterization is described in Experimental procedures.
[c]Mean numbers represent the $\log_2$ transformed ratios (experimental/baseline ± SE) generated by cross-comparing the replicate data sets of the *nhx1* line with the wild-type line.
[d]Student's *t*-test *P*-values for data comparison.

proteins involved in cytosolic protein traffic (DnaJ, clathrin coat, small heat-shock), Golgi processing (*N*-acetylglucosaminyl transferase) and protein modification (UBX) further suggest altered protein trafficking in the *nhx1* line. These results, together with the processing-related transcripts with increased expression noted in the previous section, would suggest that AtNHX1 plays a role in the regulation of vesicular trafficking components, similar to the NHX1 homolog, Nhx1p, in vesicular trafficking in yeast (Bowers *et al.*, 2000).

Absence of AtNHX1 alters transcriptional response to salt stress

In order to characterize changes in transcriptional levels induced by the growth of the wild-type and *nhx1* plants in the presence of salinity, we examined the transcriptional changes resulting from a 2-week extended exposure to 100 mM NaCl treatment of both *nhx1* and wild-type plants with control treatment for the respective plant lines providing baseline expression values. Analysis of the transcripts that are increased after 2 weeks of salt stress in these plants illustrates the differences and similarities in the adaptation (rather than the acute responses) of the two lines to a non-lethal high salt concentration and could shed light on the antiporter role(s) of AtNHX1 in this response (Figure 3a, Tables 3 and 4).

Increased expression. Several genes encoding energy-associated proteins were induced in both the wild-type (11) and knockout (16) plants grown in the presence of 100 mM NaCl (Table 3). Some of these genes were significantly enhanced in both lines (orf143, ofrX, orf114, At2g40100).

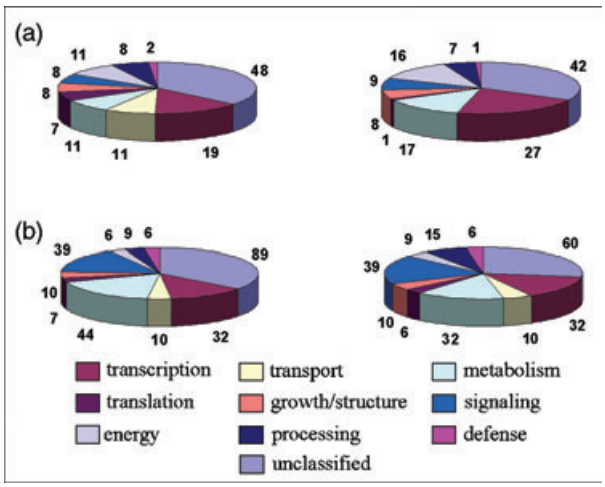

Figure 3. Relative distribution of altered transcripts in the wild-type and *nhx1* knockout lines.
(a) Transcripts displaying increased transcription levels after growing for 2 weeks in the presence of 100 mM NaCl. Left: wild-type plants; Right: *nhx1* plants.
(b) Transcripts displaying decreased transcription levels after growing for 2 weeks in the presence of 100 mM NaCl. Left: wild-type plants; Right: *nhx1* plants.
Criteria used to assign function are described in Experimental procedures.

Others were significantly increased in the knockout plants and showed similar trends of enhanced expression in the wild-type plants (At2g07695, ndhB, At5g22500, At1g31600, ycf2.1, orf153a, ycf3, At5g633030). Similarly, some genes that were significantly increased in the wild-type plants showed trends of induced expression in the *nhx1* plants (rbcL, At1g23020). The overall similarities of salt-induced trends among energy-related transcripts would suggest a commonality of salt stress adaptation between the lines, with the stronger trends in the knockout plant a result of increased salt sensitivity. However, there are some intriguing differences between the two lines. For example, the expression of a mitochondrial gene encoding subunit 2 of cytochrome oxidase (COX2) was increased in the wild-type plants whereas it appeared somewhat diminished in the knockout plants, yet the expression of a nuclear gene encoding another cytochrome *c* oxidase subunit 2 (At2g07695) was increased in the knockout plants and not in the wild-type plants. The expression of mitochondrial and nuclear genes encoding cytochrome *c* oxidase subunits was differentially regulated in Arabidopsis plants grown in the presence of metabolizable sugars or different nitrogen sources (Curi *et al.*, 2003), although an understanding of the differential expression of the two isoforms of this subunit within the same organism is still obscure. Nonetheless, our results would suggest a link between the altered ion homeostasis of the knockout plants and the differential regulation of expression of the cytochrome *c* oxidase complex subunit. Additionally, At3g15352 was significantly downregulated by salt in the *nhx1* but not in the wild-type plants. At3g15352 encodes a protein with homology to the yeast copper chaperone (Cox17) that delivers copper to the cytochrome *c* oxidase complex (Rees and Thiele, 2004 and references therein). These results further suggest that altered cellular ion homeostasis (due to the lack of AtNHX1) also affects copper-mediated processes and as a consequence organelle function.

Another interesting pattern of expression among the salt-induced energy-associated transcripts was seen with the genes encoding subunits of the chloroplast NDH complex. While two transcripts encoding subunits ndhB and ndhC significantly increased in the knockout line, with a lesser but similar pattern in the wild type, subunit ndhH only appeared to be induced by salt in the wild-type line. Previous studies have shown that under conditions that inhibited PSII and stimulated cyclic electron transport and PSI, the activity of NADH dehydrogenase increased and this increase was correlated with an increased amount of the subunit ndhH (Quiles and Lopez, 2004). The increased expression of genes encoding subunits of the NADH dehydrogenase complex in both wild-type and knockout plants can be explained by the known inhibition of PSII by salt stress (Lu and Vonshak, 2002). Nonetheless, the lack of induction of nadH suggests an effect of the altered cytosolic Na^+ content on chloroplast homeostasis during salt in the knockout plants. A further explanation for the different levels of expression of organelle transcripts may be due to the diminished expression of key regulatory elements of plastid gene expression, which will be discussed later.

The expression of genes encoding for a thioredoxin-related protein (At1g50850) and a phospholipid hydroperoxide glutathione peroxidase (AtGPX6/At4g11600) was enhanced in the wild-type plants but not in the knockout plants. Thioredoxins act as key regulators of cellular redox balance in the cell by reducing disulfide bridges of a large number of targets (Balmer *et al.*, 2004). Phospholipid hydroperoxide glutathione peroxidases are key enzymes in the protection of membranes against oxidative stress (Nakagawa and Imai, 2000) and AtGPX6, in particular, responds to a variety of abiotic stresses and hormonal treatments, particularly salt and cold (Milla *et al.*, 2003). Furthermore, transcript levels of glutathione peroxidases were enhanced during salt stress of salt-tolerant varieties of pea (Hernandez *et al.*, 2000) and tomato (Mittova *et al.*, 2002), but not in the salt-sensitive varieties. Perhaps the enhanced salt sensitivity of the *nhx1* plants (Apse *et al.*, 2003) is also the reason for the lack of induction of these transcripts within the mutant line.

In response to salt stress, the wild-type line showed the induction of 12 genes encoding transport-related proteins (Table 3) but the *nhx1* line did not show a significant induction of any transcripts in this category. The increased expression of the transporters in the wild-type line would

Table 3 Transcripts of interest with significantly increased expression as a result of salt treatment[a]

			nhx1[e]		Wild type[e]	
Functional classification[b]	Accession	Description	Mean ± SE[c]	*P*[d]	Mean ± SE[c]	*P*[d]
Transport	At1g74810	Anion transporter	0.44 ± 0.41	0.49	**1.44 ± 0.18**	**0.00**
	At3g12520	Sulfate transporter	−0.21 ± 0.15	0.23	**1.22 ± 0.21**	**0.02**
	At3g59030	Putative MATE	0.33 ± 0.51	0.47	**1.10 ± 0.14**	**0.00**
	At1g08230	Amino acid transporter family protein	0.17 ± 0.43	0.44	**1.08 ± 0.19**	**0.01**
	At2g47800	Glutathione-conjugate transporter AtMRP4	−0.13 ± 0.31	0.45	**1.06 ± 0.06**	**0.00**
	At3g53210	Nodulin MtN21 family protein	0.33 ± 0.08	0.06	**1.01 ± 0.21**	**0.03**
	At1g66760	MATE efflux family	−0.21 ± 0.28	0.39	**1.01 ± 0.19**	**0.02**
	At2g16660	Nodulin-like	0.42 ± 0.11	0.08	**0.98 ± 0.13**	**0.00**
	At1g68570	Peptide transporter	0.27 ± 0.18	0.30	**0.92 ± 0.03**	**0.00**
	At5g02270	ABC transporter-like protein NBD-like	0.27 ± 0.20	0.27	**0.92 ± 0.13**	**0.01**
	At5g65990	Amino acid transporter	0.50 ± 0.08	0.02	**0.80 ± 0.09**	**0.00**
Translation	rps14	Ribosomal protein S14	**1.92 ± 0.41**	**0.03**	**1.68 ± 0.49**	**0.03**
	At5g14610	DRH1 DEAD box-like	−0.71 ± 0.42	0.31	**1.58 ± 0.40**	**0.02**
	At1g80800	Ribosomal	−1.17 ± 0.57	0.21	**1.32 ± 0.20**	**0.01**
	At2g07734	Ribosomal protein S4 (RPS4)	0.61 ± 0.19	0.17	**1.09 ± 0.18**	**0.02**
	At5g09500	Ribosomal protein S15-like	0.94 ± 0.27	0.09	**1.05 ± 0.22**	**0.02**
	At2g27760	tRNA isopentenylpyrophosphate transferase	0.11 ± 0.15	0.32	**1.00 ± 0.19**	**0.02**
	rps11	Ribosomal protein S11	0.03 ± 0.18	0.44	**0.97 ± 0.16**	**0.01**
Energy	orf143	Hypothetical mitochondrial protein	**2.42 ± 0.25**	**0.01**	**1.34 ± 0.19**	**0.01**
	ofrX	Hypothetical mitochondrial protein	**1.24 ± 0.30**	**0.03**	**1.15 ± 0.21**	**0.02**
	orf114	Hypothetical mitochondrial protein	**1.03 ± 0.12**	**0.00**	**1.27 ± 0.17**	**0.01**
	At2g40100	Putative chlorophyll *a*/*b* binding	**0.91 ± 0.14**	**0.02**	**1.04 ± 0.18**	**0.01**
	At2g07727	Cytochrome *b*	**1.86 ± 0.39**	**0.02**	0.43 ± 0.38	0.48
	orf204	Hypothetical mitochondrial protein	**1.63 ± 0.12**	**0.00**	0.70 ± 0.25	0.07
	ndhG	NADH dehydrogenase ND6 subunit G, chloroplastic	**1.53 ± 0.30**	**0.03**	0.78 ± 0.38	0.20
	At2g07695	Cytochrome *c* oxidase subunit 2-like	**1.53 ± 0.22**	**0.01**	0.12 ± 0.15	0.42
	ndhB.1	NADH dehydrogenase ND2 subunit B.1, chloroplastic	**1.41 ± 0.30**	**0.02**	0.99 ± 0.40	0.09
	At5g22500	Male sterility 2-like, acyl CoA reductase	**1.38 ± 0.24**	**0.02**	1.26 ± 0.38	0.06
	At1g31600	Hypothetical protein predicted by genemark.hmm	**1.35 ± 0.25**	**0.03**	0.64 ± 0.25	0.15
	ycf2.1	Hypothetical chloroplast protein	**1.18 ± 0.18**	**0.02**	1.22 ± 0.53	0.12
	nad3	NADH dehydrogenase subunit 3, mitochondrial	**1.18 ± 0.23**	**0.02**	0.49 ± 0.15	0.09
	orf153a	Hypothetical mitochondrial protein	**1.10 ± 0.07**	**0.00**	0.69 ± 0.23	0.09
	ycf3	Photosystem assembly I protein	**1.03 ± 0.13**	**0.01**	1.13 ± 0.36	0.08
	At5g63030	Glutaredoxin-like	**0.85 ± 0.13**	**0.01**	0.46 ± 0.14	0.09
	rbcL	Large subunit of RUBISCO	0.83 ± 0.69	0.30	**1.82 ± 0.25**	**0.01**
	At1g23020	Superoxide-generating NADPH oxidase flavocytochrome	0.90 ± 0.46	0.33	**1.55 ± 0.37**	**0.02**
	COX2	Cytochrome *c* oxidase subunit 2, mitochondria	−0.59 ± 0.22	0.17	**1.34 ± 0.23**	**0.02**
	psbE	PSII cytochrome b559	0.31 ± 0.19	0.31	**1.31 ± 0.33**	**0.03**
	ndhH	NADH dehydrogenase subunit H, chloroplastic	0.09 ± 0.16	0.41	**1.29 ± 0.28**	**0.05**
	At1g50950	Thioredoxin-related	0.30 ± 0.21	0.17	**1.23 ± 0.13**	**0.00**
	At4g11600	Phospholipid hydroperoxide glutathione peroxidase (GPX6)	−0.07 ± 0.09	0.36	**0.95 ± 0.15**	**0.01**
Processing	At2g33735	DnaJ heat shock N-terminal domain-containing	**2.41 ± 0.42**	**0.01**	1.20 ± 0.28	0.07
	At3g44500	Ulp1 protease family	**1.52 ± 0.24**	**0.01**	0.31 ± 0.26	0.27
	At2g17880	Putative DnaJ	**1.25 ± 0.20**	**0.01**	−0.31 ± 0.50	0.27
	At3g16620	Chloroplast outer membrane, GTP-binding	**1.25 ± 0.30**	**0.01**	−0.16 ± 0.34	0.25
	At5g02370	Kinesin-like	**1.24 ± 0.30**	**0.03**	0.24 ± 0.50	0.46
	At1g47750	Peroxisomal biogenesis factor 11 family	**1.09 ± 0.24**	**0.03**	0.46 ± 0.23	0.17
	At3g11240	Arginine-tRNA-protein transferase	**0.92 ± 0.14**	**0.01**	−0.32 ± 0.19	0.20
	At3g03180	Got1-like family	−0.27 ± 0.60	0.29	**1.54 ± 0.37**	**0.04**
	At2g23000	Serine carboxypeptidase I	−0.03 ± 0.17	0.49	**1.23 ± 0.20**	**0.00**
	At5g65930	Kinesin-like calmodulin-binding protein	0.57 ± 0.19	0.11	**1.13 ± 0.19**	**0.02**
	At5g65370	Epsin N-terminal homology (ENTH) domain	0.99 ± 0.39	0.11	**1.08 ± 0.19**	**0.02**
	At4g04670	*S*-adenosylmethionine-dependent methyltransferase	0.45 ± 0.24	0.18	**1.05 ± 0.16**	**0.02**
	At2g24640	Ubiquitin carboxyl terminal hydrolase	1.11 ± 0.47	0.19	**0.99 ± 0.11**	**0.00**
	At3g55150	Leucine zipper, Exo70 exocyst complex subunit	−0.31 ± 0.13	0.16	**0.98 ± 0.10**	**0.00**
	At4g33090	Aminopeptidase-like	−0.15 ± 0.09	0.21	**0.68 ± 0.04**	**0.00**

Table 3 (*Continued*)

Functional classification[b]	Accession	Description	*nhx1*[e] Mean ± SE[c]	*nhx1*[e] *P*[d]	Wild type[e] Mean ± SE[c]	Wild type[e] *P*[d]
Growth/structure	At5g59320	Lipid-transfer, LPT3	**1.24 ± 0.17**	**0.03**	**3.07 ± 0.40**	**0.01**
	At1g10640	Polygalacturonase PG1	**1.60 ± 0.33**	**0.01**	0.74 ± 0.15	0.02
	At1g77410	β-Galactosidase	**1.32 ± 0.22**	**0.02**	−0.05 ± 0.13	0.46
	At4g12510	pEARLI 1-like	**1.17 ± 0.20**	**0.01**	−0.02 ± 0.18	0.47
	At2g03220	Xyloglucan fucosyltransferase AtFT1	**0.93 ± 0.15**	**0.01**	0.33 ± 0.13	0.13
	At4g26750	Putative extensin precursor	**0.91 ± 0.05**	**0.00**	0.31 ± 0.07	0.04
	At5g09530	Periaxin-like	−0.19 ± 0.61	0.36	**2.92 ± 0.60**	**0.02**
	At4g16590	Cellulose synthase-like	−0.75 ± 0.27	0.13	**2.45 ± 0.26**	**0.01**
	At1g02205	Lipid transfer protein (CER1)	0.96 ± 0.24	0.03	**1.47 ± 0.28**	**0.02**
	At3g23670	Kinesin-like	0.24 ± 0.24	0.25	**1.23 ± 0.19**	**0.01**
	At1g26770	Expansin 10	0.44 ± 0.18	0.21	**1.16 ± 0.13**	**0.00**
	At1g15570	Putative cyclin	−0.22 ± 0.14	0.22	**0.94 ± 0.13**	**0.01**
	At1g48750	Lipid transfer	0.60 ± 0.13	0.05	**0.81 ± 0.08**	**0.00**
	At4g33090	Aminopeptidase-like	−0.15 ± 0.09	0.21	**0.68 ± 0.04**	**0.00**

[a]The complete table of the 226 transcripts with increased expression as a result of salt treatment can be found in Table S3.
[b]Functional characterization is described in Experimental procedures.
[c]Mean numbers represent the $\log_2$ transformed ratios (experimental/baseline ± SE) generated by cross-comparing the replicate data sets of salt-treated transcript levels with control treatment levels for the respective plant line.
[d]Student's *t*-test *P*-values for data comparison.
[e]Transcript changes that met both statistical criteria for the respective comparison are highlighted in bold.

suggest roles in the salt response and maintenance of ion homeostasis. The lack of induction of these genes in the *nhx1* plants likely reflects a compromised capacity to maintain a high vacuolar ion concentration during salt stress as a result of the absent antiporter. Only two of theses transcripts, encoding a nodulin-like protein and an amino acid transporter (Table 3), showed a trend of salt induction in the *nhx1* line (supported by relatively low standard error and *P*-values). The other transport-related transcripts induced in the wild-type line by salt did not show meaningful changes in patterns of gene expression in the knockout line. Notably, there was no significant induction of AtNHX1 in the wild-type or other Na^+ transporters in either plant line in response to salt stress. These results contrast those reported earlier showing the induction of *AtNHX1* by salt (Shi and Zhu, 2002). This apparent difference is most likely due to the different experimental conditions used. Shi and Zhu (2002) grew the plants in agar plates in a high K^+ medium and the plants were exposed to lethal salt concentrations for 5 h. In the present study, plants were grown in pots with a low K^+ medium and exposed to sub-lethal salinity levels for 2 weeks. As a result the transporters induced here are representative of a more adaptive response of wild-type Arabidopsis to long-term stress, and the absence of significant transporter inductions in the *nhx1* line suggests that the lack of functional AtNHX1 effects a different overall adaptive response to salt stress beyond the increased movement of ions across membrane barriers. Most of these transporters appear to be already increased (at least somewhat) in the *nhx1* line even in the absence of salt stress (data not shown) suggesting that the mutant plants had already compensated to the stress conditions caused by ionic imbalance, and increasing the salt stress did not engender further significant change.

Among the transcripts encoding genes for proteins putatively associated with protein processing and modification, the wild-type and the *nhx1* mutant plant lines displayed notably different trends of induction as a consequence of salt stress (Table 3). Of the seven transcripts in this category that were significantly induced by salt in *nhx1*, only At2g33735 (containing a DnaJ N-terminal domain) was also increased in both the *nhx1* and wild-type plants by salt. On the contrary, of the eight processing transcripts induced by salt in the wild type, at least three showed a similar pattern, albeit moderate, in the knockout line as well. These transcripts encode a kinesin-like calmodulin-binding protein (At5g65930), a ubiquitin carboxyl terminal hydrolase (At2g24640), and a protein (At5g65370) with an ENTH domain [PF01417] related to clathrin assembly different than the protein with the same domain described earlier (At2g43160, Table 2) that had higher expression in the *nhx1* line under controlled conditions. These changes further implicate AtNHX1 as an important component influencing cellular trafficking and processing.

Decreased expression. A number of genes displayed a significant decrease in expression in both wild-type (235) and *nhx1* knockout (206) plants exposed to salt stress (Table 4,

Table 4 Transcripts of interest with significantly decreased expression as a result of salt treatment[a]

			nhx1[e]		Wild type[e]	
Functional classification[b]	Accession	Description	Mean ± SE[c]	*P*[d]	Mean ± SE[c]	*P*[d]
Transcription	At5g07100	WRKY SPF1-like	**−2.78 ± 0.26**	**0.04**	−0.49 ± 0.40	0.20
	At4g18170	SPF1 DNA binding-like, WRKY domain	**−2.53 ± 0.45**	**0.04**	0.04 ± 0.44	0.34
	At4g24240	WRKY3	**−1.16 ± 0.16**	**0.03**	0.09 ± 0.25	0.45
	At4g31800	WRKY	**−0.99 ± 0.08**	**0.00**	−0.28 ± 0.21	0.34
Transport	At5g46240	Potassium channel protein KAT1	**−0.93 ± 0.14**	**0.03**	**−1.07 ± 0.19**	**0.01**
	At5g20380	Na+-dependent inorganic phosphate cotransporter like	**−2.38 ± 0.25**	**0.02**	−1.13 ± 0.45	0.22
	At2g34350	Nodulin-like	**−1.87 ± 0.33**	**0.03**	−0.73 ± 0.34	0.19
	At5g26330	Putative metal transporter	**−1.39 ± 0.29**	**0.04**	−0.49 ± 0.32	0.28
	At4g24120	Peptide transporter	**−1.37 ± 0.24**	**0.03**	−0.67 ± 0.25	0.12
	At2g19600	Potassium:hydrogen antiporter KEA4	**−1.34 ± 0.29**	**0.03**	−0.03 ± 0.53	0.42
	At1g06470	Phosphate/glucose-phosphate translocator-like	**−1.23 ± 0.27**	**0.03**	−0.18 ± 0.09	0.20
	At4g21910	MATE-like	**−1.21 ± 0.18**	**0.04**	0.41 ± 0.20	0.19
	At1g44100	AAP5, proton/amino acid cotransporter	**−1.02 ± 0.19**	**0.02**	−0.32 ± 0.15	0.19
	At4g18910	Putative MIP, nodulin-26-like	**−0.80 ± 0.10**	**0.02**	−0.60 ± 0.32	0.26
	At5g52760	Heavy metal-associated domain-containing	−0.27 ± 0.43	0.32	**−1.65 ± 0.16**	**0.01**
	At2g39210	Nodulin-like	−1.20 ± 0.21	0.08	**−1.58 ± 0.21**	**0.04**
	At1g05300	Putative zinc transporter	−1.55 ± 0.40	0.15	**−1.46 ± 0.23**	**0.04**
	At5g45380	Urea active transporter-like	−0.43 ± 0.18	0.14	**−1.32 ± 0.22**	**0.04**
	At1g12110	CHL1, nitrate transporter	−0.44 ± 0.27	0.24	**−1.21 ± 0.16**	**0.01**
	At1g28220	PUP3, purine permease	−0.25 ± 0.31	0.29	**−1.11 ± 0.19**	**0.01**
	At5g17860	Potassium-dependent sodium–calcium exchanger-like, CAX7	0.12 ± 0.32	0.42	**−1.08 ± 0.15**	**0.02**
	At3g48970	GMFP7 isoprenylated-like	0.47 ± 0.26	0.29	**−1.03 ± 0.13**	**0.01**
	At4g17340	MIP-like	−0.24 ± 0.10	0.17	**−0.76 ± 0.08**	**0.01**
Metabolism	At1g01190	Cytochrome P450-like	**−1.99 ± 0.28**	**0.05**	**−2.44 ± 0.30**	**0.00**
	At2g46720	Putative β-ketoacyl CoA synthase	**−1.36 ± 0.21**	**0.03**	**−1.52 ± 0.22**	**0.01**
	At5g37600	Glutamate-ammonia ligase	**−1.10 ± 0.16**	**0.02**	**−1.04 ± 0.18**	**0.03**
	At1g13080	Cytochrome P450 monooxygenase	**−0.89 ± 0.15**	**0.02**	**−1.09 ± 0.18**	**0.02**
	At1g31700	Copper amine oxidase	**−2.74 ± 0.56**	**0.03**	−0.21 ± 0.34	0.35
	At3g43670	Amine oxidase-like	**−1.33 ± 0.21**	**0.03**	0.25 ± 0.12	0.19
	At5g16570	Glutamine biosynthesis	**−1.32 ± 0.14**	**0.00**	−1.13 ± 0.28	0.03
	At1g31680	Copper amine oxidase	**−1.11 ± 0.14**	**0.02**	0.78 ± 0.41	0.29
	At2g29420	Glutathione S-transferase	−0.89 ± 0.44	0.16	**−1.07 ± 0.18**	**0.04**
	At2g16060	Class 1 non-symbiotic hemoglobin (AHB1)	0.45 ± 0.14	0.10	**−1.05 ± 0.22**	**0.03**
	At1g27130	Glutathione transferase	−0.43 ± 0.06	0.01	**−1.04 ± 0.09**	**0.00**
	At3g24090	Glutamine:fructose-6-phosphate amidotransferase	−0.85 ± 0.29	0.14	**−1.02 ± 0.15**	**0.01**
Signaling	At1g75010	MORN repeat/phosphatidylinositol-4-phosphate 5-kinase	**−2.14 ± 0.53**	**0.02**	0.39 ± 0.21	0.12
	At4g21380	Receptor-like serine/threonine protein kinase ARK3	**−1.17 ± 0.15**	**0.01**	−0.31 ± 0.15	0.16
	At3g59400	GUN4, genomes uncoupled	**−1.10 ± 0.15**	**0.02**	−0.20 ± 0.32	0.42
	At3g46790	CRR2, chlororespiratory reduction 2	**−0.82 ± 0.09**	**0.01**	0.30 ± 0.14	0.19
Energy	At1g03850	Glutaredoxin-like	**−3.52 ± 0.46**	**0.00**	**−2.29 ± 0.19**	**0.00**
	At3g62950	Glutaredoxin-like	**−2.16 ± 0.34**	**0.01**	−0.75 ± 0.31	0.13
	At1g06830	Glutaredoxin-like	−0.90 ± 0.24	0.06	**−1.64 ± 0.17**	**0.01**
	At4g15680	Glutaredoxin	−0.90 ± 0.24	0.10	**−0.94 ± 0.18**	**0.02**
	At3g15352	Copper chaperone	**−1.46 ± 0.24**	**0.00**	−0.52 ± 0.05	0.001
Processing	At4g01390	MATH domain-containing	**−2.51 ± 0.34**	**0.01**	−0.97 ± 0.49	0.15
	At4g20110	Vacuolar sorting receptor-like BP-80	**−1.30 ± 0.21**	**0.05**	−0.99 ± 0.48	0.18
	At2g43160	Putative clathrin-binding (epsin) ENTH, extensin domains	**−1.30 ± 0.22**	**0.02**	0.27 ± 0.26	0.42
	At1g18320	Preprotein translocase-like	**−1.29 ± 0.18**	**0.03**	0.11 ± 0.24	0.36
	At4g00930	COP1-interacting protein 4.1	**−1.29 ± 0.20**	**0.02**	1.06 ± 0.44	0.15
	At5g06910	DnaJ homolog	**−1.28 ± 0.15**	**0.02**	−0.43 ± 0.12	0.10
	At3g17970	Chloroplast outer membrane translocon subunit, amidase-like	**−1.16 ± 0.06**	**0.00**	0.68 ± 0.24	0.11
	At2g45690	Shrunken seed (SSE1), peroxisome biogenesis factor 16-like	**−1.16 ± 0.21**	**0.03**	−0.12 ± 0.40	0.35
	At1g15000	Serine carboxypeptidase precursor	**−1.15 ± 0.16**	**0.01**	0.06 ± 0.16	0.50
	At5g66960	Protease-like	**−1.14 ± 0.17**	**0.03**	−0.33 ± 0.29	0.40
	At1g68370	ARG1 (Altered Response to Gravity), DnaJ-like	**−1.09 ± 0.21**	**0.01**	−0.90 ± 0.27	0.07
	At2g39710	Aspartyl protease family	**−1.04 ± 0.11**	**0.02**	−0.22 ± 0.16	0.26

Table 4 (*Continued*)

Functional classification[b]	Accession	Description	*nhx1*[e] Mean ± SE[c]	*nhx1*[e] P[d]	Wild type[e] Mean ± SE[c]	Wild type[e] P[d]
	At5g59730	Exocyst subunit EXO70 family, leucine zipper-containing	**−0.95 ± 0.12**	**0.01**	−0.30 ± 0.21	0.28
	At4g20410	Gamma-SNAP	**−0.94 ± 0.17**	**0.02**	−0.32 ± 0.14	0.15
	At2g35635	Ubiquitin-like (UBQ7)	**−0.83 ± 0.05**	**0.00**	−0.02 ± 0.15	0.41
	At5g26280	MATH domain-containing	−0.48 ± 0.36	0.18	**−1.79 ± 0.40**	**0.02**
	At2g21540	Putative phosphatidylinositol phophatidylcholine transfer	−0.38 ± 0.09	0.04	**−1.25 ± 0.29**	**0.04**
	At3g55470	Elicitor responsive/phloem-like FlERG2	−0.73 ± 0.15	0.03	**−1.25 ± 0.30**	**0.04**
	At3g02980	Putative *N*-acetlytransferase	−0.18 ± 0.27	0.50	**−1.12 ± 0.13**	**0.01**
	At1g69020	Similar to protease II (oligopeptidase B)	0.14 ± 0.20	0.40	**−1.11 ± 0.20**	**0.02**
	At1g71300	ARE1-like	0.25 ± 0.12	0.15	**−1.04 ± 0.18**	**0.02**
	At1g73330	Dr4 (protease inhibitor)	−0.05 ± 0.11	0.37	**−0.97 ± 0.11**	**0.01**
	At2g05320	Putative *N*-acetylglucosaminyltransferase	0.21 ± 0.28	0.29	**−0.86 ± 0.09**	**0.01**
	At3g61060	F-box family/lectin-related	0.18 ± 0.15	0.32	**−0.72 ± 0.04**	**0.00**
Growth/structure	At1g05320	Myosin-related	**−0.96 ± 0.11**	**0.01**	**−0.93 ± 0.13**	**0.03**
	At2g20290	Putative myosin heavy chain	**−1.83 ± 0.22**	**0.03**	0.28 ± 0.27	0.34
	At1g59540	Kinesin motor (kin2)	**−1.57 ± 0.40**	**0.04**	0.19 ± 0.70	0.36
	At1g76930	Extensin 4	**−1.52 ± 0.29**	**0.05**	−0.90 ± 0.32	0.16
	At5g67100	DNA polymerase alpha 1	**−1.49 ± 0.24**	**0.01**	−0.46 ± 0.11	0.08
	At5g44930	Exostosin domain	**−1.40 ± 0.16**	**0.02**	−1.08 ± 0.34	0.12
	At1g50010	Tubulin alpha-2/alpha-4 chain	**−1.00 ± 0.13**	**0.01**	−0.46 ± 0.05	0.00
	At2g20960	pEARLI 4	**−0.97 ± 0.11**	**0.005**	−0.12 ± 0.18	0.377
	At3g25540	Longevity-assurance (LAG1) family	**−0.94 ± 0.17**	**0.01**	−0.15 ± 0.11	0.29
	At4g28250	β-Expansin/allergen	**−0.88 ± 0.14**	**0.02**	0.37 ± 0.17	0.20
	At4g12480	pEARLI1	−3.00 ± 0.50	0.14	**−1.67 ± 0.18**	**0.01**
	At5g56870	β-Galactosidase	−1.25 ± 0.29	0.12	**−1.66 ± 0.27**	**0.04**
	At2g15390	Xyloglucan fucosyltransferase	−0.90 ± 0.26	0.14	**−1.49 ± 0.18**	**0.03**
	At1g02640	β-Xylosidase	−0.03 ± 0.22	0.41	**−1.10 ± 0.21**	**0.04**
	At5g48070	Xyloglucan endo-1,4-β-D-glucanase	0.47 ± 0.31	0.34	**−1.10 ± 0.22**	**0.04**
	At4g12470	pEARLI1-like	−1.90 ± 0.51	0.16	**−1.02 ± 0.16**	**0.03**
	At1g05320	Myosin-related	−0.96 ± 0.11	0.01	**−0.93 ± 0.13**	**0.03**
	At4g12730	Fasciclin-like arabinogalactan protein	−0.65 ± 0.06	0.00	**−0.90 ± 0.07**	**0.00**
	At1g47230	Cyclin-like	0.33 ± 0.09	0.09	**−0.84 ± 0.07**	**0.00**
	At2g45180	Protease inhibitor/seed storage/ lipid transfer family	−0.08 ± 0.06	0.28	**−0.67 ± 0.04**	**0.00**

[a]The complete table of the 421 transcripts with increased expression due to salt treatment can be found in Table S4.
[b]Functional characterization is described in Experimental procedures.
[c]Mean numbers represent the $\log_2$ transformed ratios (experimental/baseline ± SE) generated by cross-comparing the replicate data sets of salt-treated transcripts levels with control treatment levels for the respective plant line.
[d]Student's *t*-test *P*-values for data comparison.
[e]Transcript changes that met both statistical criteria for the respective comparison are highlighted in bold.

Tables S5 and S6). These genes displayed a similar functional breakdown (Figure 3), suggesting that there was a similar overall response of decreased gene expression. However, as will be discussed later, there was little overlap of significantly downregulated transcripts.

Of the diminished transport-related transcripts, most of those that were significantly downregulated by salt in the wild type showed a similar but less significant trend of downregulation in the *nhx1* line. Additionally, of the transport-related transcripts significantly diminished in the *nhx1* line, four showed a similar trend in the wild-type plants (Table 4). There were a few salt-diminished transport-related transcripts that showed notably different profiles between the two lines. For example, a putative potassium-dependent sodium–calcium exchanger (CAX7/At5g17860) was significantly reduced in the wild-type line, but did not change as a result of salt treatment in the *nhx1* line. In addition, of the transcripts downregulated during salt stress in the *nhx1* line that did not display a similar trend in wild-type salt-treated plants were a putative metal transporter gene (At5g26330), an integral membrane phosphate translocator gene (At1g06470), and a putative potassium-proton antiporter (KEA4/At2g19600) belonging to the CPA2 family of Arabidopsis cation/proton antiporters (Mäser *et al.*, 2001).

Only one transcript encoding a putative member of the multi antibacterial extrusion (MATE) family [PF01554] of transporters (At4g21910) appeared to be significantly downregulated in the *nhx1* line because of salt and yet had a trend of upregulation because of salt in the wild type.

The wild-type and *nhx1* lines showed significantly diminished expression of 32 transcription-related transcripts each (Table S4). Four transcripts encoding proteins containing WRKY domains [PF03106], shown to play key roles in both biotic and abiotic stress (Eulgem *et al.*, 2000), were downregulated only in the *nhx1* plants (Table 4). The further significance of diminished transcription of the different transcription-related genes and how these differences reflect the altered phenotype and increased salt sensitivity of the *nhx1* line is out of the scope of this report, but could lead to future studies of these transcription factors in terms of their contribution to cellular homeostasis.

In the wild type, the structure-related transcripts that were significantly decreased appear primarily related to processes that modify the cell wall and other exterior components of cell structure. The trends of altered expression in the salt-treated *nhx1* line suggested diminished expression for these same genes, again supporting a similar, yet weaker (less significant), salt response in the mutant line. In addition, the *nhx1* line showed a significant reduction of a handful of other structure-related transcripts, although the encoded proteins appear to instead contribute primarily to internal cellular structure and organization, including a tubulin (At1g50010), a heavy chain myosin (At2g20290), and a kinesin motor (At1g59540). Only the tubulin transcript also showed a weakly similar trend of reduced expression in the wild type because of salt. Overall this suggests that the internal components of cell structure were more affected by salt stress in the *nhx1* line compared with the wild type. Among the 'exterior' structure-related transcripts, the mutant line also displayed a significant reduction in the expression of genes encoding a β-expansin (At4g28250) and an extensin (AtEXT1/AtEXT4/At1g76930). Expansins are key regulators of cell wall extension during growth (Li *et al.*, 2003) and the overexpression of expansins increased the growth of the transgenic plants (Cho and Cosgrove, 2000). In Arabidopsis, the expression of AtEXT2 was suppressed by salt stress and the expression of AtEXT4 was partially inhibited (Yoshiba *et al.*, 2001). The inhibition of a β-expansin and an extensin in *nhx1* would result in decreased expansion and increased secondary wall formation, perhaps contributing to the altered phenotype (reduced leaf and cell size, increased salt sensitivity) of the *nhx1* knockout plants (Apse *et al.*, 2003).

One signaling transcript that was significantly downregulated by salt in *nhx1*, but not significantly altered in the wild type, encodes GUN4/At3g59400. GUN4 participates in plastid-to-nucleus signaling by regulating Mg-protoporphyrin IX, an intermediate in chloroplast biosynthesis (Larkin *et al.*, 2003). Additionally, downregulated by salt in *nhx1*, but appearing slightly upregulated in the wild-type line, was CRR2/At3g46790, a gene whose function as a molecular switch regulates the expression of the chloroplast NDH complex, specifically ndhB (Hashimoto *et al.*, 2003). The salt-dependent differences in CRR2 expression in the *nhx1* plants, together with the upregulation of the chloroplast NDH complex subunits (Table 3), support the possible effect(s) of altered ion homeostasis on nucleus–chloroplast communication.

A number of processing-related transcripts were significantly reduced during salt stress in *nhx1* but were not significantly altered in the wild type (although several showed similar trends). Included among these are a DnaJ-domain [PF00226] protein (ARG1/At1g68370) that has been implicated to play an important role in gravitropism and potentially interact with the cytoskeleton (Sedbrook *et al.*, 1999), a putative DnaJ protein (AtJ6/At5g06910), a γ-SNAP [PF02071] protein (At4g20410) involved in intracellular membrane fusion and vesicular trafficking (Stenbeck, 1998), and a vacuolar sorting receptor (AtELP3/At4g20110) that is involved in the transport of vacuolar proteins (Ahmed *et al.*, 2000), a putative clathrin-binding protein with ENTH [PF01417] and proline extensin [PF04554] domains (At2g43160), a mitochondrial import inner membrane translocase subunit family [PF02466] member (At1g18320), a COP1-interacting (CIP4/At4g00930) that promotes photomorphogenesis (Yamamoto *et al.*, 2001), and a protein (SSE1/At2g45690) that is required for protein and oil body biogenesis and plays a role in the transport of plasma membrane and cell wall-associated proteins (Lin *et al.*, 1999) (Table 4). Although the regulation of intravesicular trafficking in plants by cellular ion homeostasis is not yet clear, the downregulation of transcripts encoding proteins that are part of intracellular trafficking in the knockout plants emphasizes the importance of AtNHX1 in these processes.

Lack of overlap between comparisons highlights the role of AtNHX1

There was very little overlap between the comparisons that were analyzed for this study. The number of significantly affected transcripts had no more than 6% in common between any given comparison (Figure 4), and because of this low percentage, it could be argued that some of these overlapping transcripts represent statistical outliers. Nevertheless, it is possible that these transcripts and/or their products have important roles related to AtNHX1 and/or to salt response. All of the overlapping salt-responsive transcripts that changed significantly in both wild-type and knockout lines displayed similar trends with respect to control treatments (with only one exception, see below). This correlation would assert that the

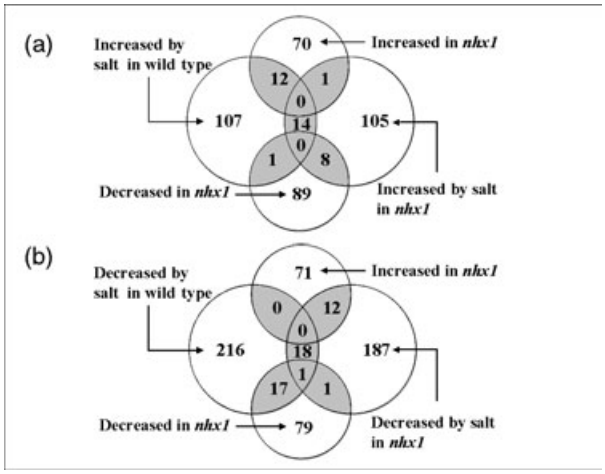

Figure 4. Venn diagrams showing the overlap of transcripts among comparisons.
(a) Transcripts displaying significantly increased levels of expression in response to 2 weeks of salt treatment in both the wild-type plants (left circle) and the *nhx1* plants (right circle) and the number of transcripts that overlap for these comparisons (shaded areas). The bottom and top circles correspond to transcripts that have increased or decreased levels of expression, respectively, in the *nhx1* plants compared with the wild-type plants grown under control conditions.
(b) A similar comparison of the transcripts that displayed decreased expression levels in response to salt. The transcripts found in the overlapping shaded areas are listed in Table 5.

differences seen were not due primarily to chance, but rather due to real changes caused by a similar stress treatment. Although the significance of all the commonly affected, overlapping transcripts, remains to be determined, the following discussion intends to highlight some of the key overlapping transcripts found.

Transcripts affected by salt independently of AtNHX1. Transcripts that are altered by salt stress conditions in both plant lines would indicate that the response of these transcripts to stress was independent of AtNHX1. Only 14 and 18 transcripts were significantly increased or decreased, respectively, by salt in both lines. This low percentage of overlapping transcripts suggests that the absence of AtNHX1 dramatically altered the response of the plants to salt. Among the transcripts that increased, a non-specific lipid transfer protein (LPT3/At5g59320) (Table 5) appears to be secreted to the cell wall and induced by ABA treatment (Arondel *et al.*, 2000) and salt (Jung *et al.*, 2003). Other putative lipid-transfer proteins were either increased or decreased (Tables 3 and 4) by salt, yet only one (pEARLI1-like/At4g12510 – increased in *nhx1*) did not show a corresponding trend between the lines. Lipid transfer proteins have been implicated in many processes such as membrane augmentation, signaling, cell wall and wax assembly, and defense mechanisms (Arondel *et al.*, 2000 and references therein), although their role during salt stress is not yet clear.

Another overlapping salt-induced gene (WOX2/At5g59340) (Table 5) is similar to the homeobox transcription factor WUSCHEL (WUS/At2g17950) and may therefore be playing a role in development and/or organ identity processes such as the transition to flowering (Lenhard *et al.*, 2002). Although the significance of this transcript to Arabidopsis seedling and the response to salt is uncertain, WOX2 is functionally required for the correct development of the embryonic apical domain (Haecker *et al.*, 2004). The increase in WOX2 expression could be related to the early flowering seen in both wild-type and knockout plants under salt stress (Apse *et al.*, 2003). Also induced in both lines were transcripts encoding a putative calcium-binding EF-hand protein (RD20/At2g33380) (Table 5) induced by abiotic stress (Takahashi *et al.*, 2000). The putative role of RD20 during salt stress is not clear; nevertheless, its induction indicates the stress response imposed by the presence of 100 mM NaCl in the growth medium.

The increase in transcription of a glyoxalase I (lactoylglutathione lyase) family [PF00903] gene (At2g28420) seen in both lines (Table 5) is supported by previous studies that have shown the upregulation of this enzyme due to salt stress in tomato (Espartero *et al.*, 1995). Moreover, its overexpression in tobacco conferred salt tolerance to the transgenic plants and its role during salt stress most likely contributes to detoxification of active oxygen species (enhancing glutathione levels) generated during stress (Singla-Pareek *et al.*, 2003). Several glutaredoxin-like and glutathione transferase-like transcripts were downregulated, either significantly in both lines, or significant in one line with a similar trend in the other line, and only one glutaredoxin-like was enhanced in both lines (Tables 3, 4 and 5). Glutathione pools are under homeostatic control, and glutathione redox state appears to be constant in leaves (Noctor *et al.*, 2002, and references therein). Thus, the significance of this differential expression is difficult to determine at this point. However, the similarity of the response in both plant lines would suggest an adjustment to salt stress that occurs independently of AtNHX1. On the contrary, two transcripts encoding a glutathione-conjugate transporter (AtMRP4/At2g47800) and a phospholipid hydroperoxide glutathione peroxidase (AtGPX6/At4g11600) were significantly upregulated in the wild-type and not in the knockout plants (Table 3). The latter protein responds to a variety of abiotic stress and hormonal treatments (Milla *et al.*, 2003). Perhaps the altered status of the *nhx1* line causes the differential expression of these stress-related transcripts, although a more direct interaction cannot be ruled out and may merit further investigation.

Eighteen transcripts were downregulated by salt in both lines (Table 5) and the encoded proteins have a variety of functional roles, although their specific roles in the salt

Table 5 Transcripts with overlapping significant changes

		Control treatments[c,d]		*nhx1* salt-treated[c,e]		Wild-type salt-treated[c,f]	
Accession	Description	Mean ± SE[a]	P^b	Mean ± SE[a]	P^b	Mean ± SE[a]	P^b
Increased because of salt in both Atnhx1 and wild type							
At3g44070	Unclassified	−0.17 ± 0.19	0.37	**1.20 ± 0.26**	**0.04**	**1.31 ± 0.15**	**0.00**
At1g47400	Unclassified	0.27 ± 0.39	0.34	**1.38 ± 0.32**	**0.01**	**2.05 ± 0.34**	**0.00**
At5g24570	Unclassified	0.08 ± 0.19	0.49	**0.99 ± 0.12**	**0.00**	**1.29 ± 0.20**	**0.00**
At5g28790	Unclassified	−0.33 ± 0.15	0.20	**1.13 ± 0.20**	**0.02**	**1.05 ± 0.20**	**0.05**
At5g59340	Wuschel protein-like	−0.77 ± 0.30	0.17	**1.34 ± 0.32**	**0.04**	**0.98 ± 0.17**	**0.01**
At5g59320	Lipid-transfer, LPT3	0.21 ± 0.29	0.41	**1.24 ± 0.17**	**0.03**	**3.07 ± 0.40**	**0.01**
At2g28420	Lactoylglutathione lyase/glyoxalase I families	0.06 ± 0.23	0.48	**1.33 ± 0.20**	**0.01**	**1.05 ± 0.22**	**0.03**
rps14	Ribosomal (chloroplast)	−0.40 ± 0.51	0.27	**1.92 ± 0.41**	**0.03**	**1.68 ± 0.49**	**0.03**
At3g09080	Transducin/WD-40 repeat families	0.15 ± 0.28	0.42	**1.10 ± 0.24**	**0.05**	**1.20 ± 0.26**	**0.04**
At2g33380	Calcium-binding EF-hand	−0.63 ± 0.07	0.00	**0.90 ± 0.15**	**0.02**	**1.20 ± 0.06**	**0.00**
orf114	Hypothetical (mitochondrial)	0.21 ± 0.15	0.27	**1.03 ± 0.12**	**0.00**	**1.27 ± 0.17**	**0.01**
orf143	Hypothetical (mitochondrial)	−0.69 ± 0.15	0.05	**2.42 ± 0.25**	**0.01**	**1.34 ± 0.19**	**0.01**
ofrX	Hypothetical (mitochondrial)	−0.27 ± 0.27	0.39	**1.24 ± 0.30**	**0.03**	**1.15 ± 0.21**	**0.02**
At2g40100	Chlorophyll *a*/*b* binding	−0.09 ± 0.17	0.34	**0.91 ± 0.14**	**0.02**	**1.04 ± 0.18**	**0.01**
Increased in Atnhx1 control and increased in the wild type with salt							
At4g36780	Unclassified	**1.09 ± 0.09**	**0.00**	−0.01 ± 0.10	0.49	**1.17 ± 0.12**	**0.00**
At1g36230	Unclassified	**2.27 ± 0.25**	**0.00**	0.69 ± 0.28	0.11	**2.31 ± 0.33**	**0.02**
At1g71900	Unclassified	**0.93 ± 0.13**	**0.00**	−0.92 ± 0.30	0.07	**0.90 ± 0.15**	**0.01**
At2g17440	Unclassified	**1.91 ± 0.34**	**0.01**	−0.30 ± 0.18	0.23	**1.56 ± 0.38**	**0.04**
At5g43160	Unclassified	**0.96 ± 0.18**	**0.03**	−0.10 ± 0.17	0.46	**1.23 ± 0.22**	**0.02**
At1g16190	Putative DNA repair protein RAD23	**0.92 ± 0.14**	**0.02**	0.43 ± 0.15	0.13	**0.98 ± 0.14**	**0.01**
At2g16660	Nodulin-like	**1.06 ± 0.14**	**0.01**	0.42 ± 0.11	0.08	**0.98 ± 0.13**	**0.00**
At5g14610	DRH1 DEAD box protein	**1.27 ± 0.34**	**0.04**	−0.71 ± 0.42	0.31	**1.58 ± 0.40**	**0.02**
At3g55150	Exocyst subunit EXO70 family	**0.87 ± 0.10**	**0.00**	−0.31 ± 0.13	0.16	**0.98 ± 0.10**	**0.00**
At3g23670	Kinesin-like	**1.33 ± 0.16**	**0.00**	0.24 ± 0.24	0.25	**1.23 ± 0.19**	**0.01**
At5g46470	Disease resistance (TIR-NBS-LRR class)	**2.13 ± 0.31**	**0.00**	0.07 ± 0.24	0.32	**1.85 ± 0.43**	**0.03**
Increased in Atnhx1 control and further increased with salt treatment							
At5g19890	Peroxidase ATP N	**0.86 ± 0.13**	**0.02**	**1.07 ± 0.14**	**0.00**	0.80 ± 0.15	0.04
Decreased in Atnhx1 control but increased in the wild type with salt							
At3g28270	At14a-like	**−1.39 ± 0.27**	**0.04**	−0.66 ± 0.27	0.19	**1.46 ± 0.31**	**0.04**
Decreased in Atnhx1 but increased with salt							
At1g73177	Unclassified	**−1.24 ± 0.12**	**0.00**	**0.95 ± 0.13**	**0.01**	−0.14 ± 0.09	0.25
At2g16590	Unclassified	**−1.02 ± 0.18**	**0.04**	**1.93 ± 0.22**	**0.01**	0.66 ± 0.20	0.11
At2g20500	Unclassified	**−0.94 ± 0.15**	**0.02**	**1.40 ± 0.21**	**0.02**	0.05 ± 0.10	0.48
At1g16640	Transcriptional factor B3 family	**−1.30 ± 0.19**	**0.01**	**1.79 ± 0.24**	**0.01**	−1.08 ± 0.29	0.06
At5g45700	NLI interacting factor	**−1.43 ± 0.32**	**0.04**	**1.64 ± 0.33**	**0.01**	0.29 ± 0.22	0.32
At2g36480	Zinc finger (C2H2-type) family protein	**−1.09 ± 0.20**	**0.02**	**1.08 ± 0.22**	**0.02**	0.05 ± 0.14	0.41
At2g19380	RNA recognition	**−0.98 ± 0.17**	**0.02**	**1.10 ± 0.13**	**0.00**	−0.38 ± 0.19	0.16
At4g33790	Putative acyl CoA reductase, male sterility 2-like	**−1.27 ± 0.20**	**0.01**	**1.47 ± 0.23**	**0.01**	−0.10 ± 0.14	0.37
Decreased because of salt in both Atnhx1 and wild type							
At1g29440	Auxin-induced	−0.25 ± 0.17	0.24	**−0.96 ± 0.18**	**0.03**	**−3.93 ± 0.32**	**0.00**
At3g49640	Putative nitrogen regulation protein (NIFR3)	0.13 ± 0.16	0.33	**−1.84 ± 0.34**	**0.03**	**−1.20 ± 0.21**	**0.02**
At5g47050	Similarity to S-ribonuclease binding	−0.42 ± 0.10	0.06	**−1.21 ± 0.30**	**0.04**	**−1.40 ± 0.12**	**0.00**
At5g23510	Unclassified	0.25 ± 0.21	0.34	**−1.22 ± 0.19**	**0.03**	**−1.60 ± 0.20**	**0.03**
At5g52120	Lectin-like	−0.67 ± 0.13	0.03	**−1.79 ± 0.14**	**0.00**	**−1.43 ± 0.21**	**0.01**
At2g21650	myb family transcription factor	−0.27 ± 0.23	0.42	**−2.72 ± 0.27**	**0.02**	**−3.06 ± 0.11**	**0.00**
At5g23690	PolyA polymerase-like	−0.19 ± 0.17	0.42	**−2.61 ± 0.26**	**0.02**	**−1.76 ± 0.17**	**0.00**
At5g23710	RNA polymerase subunit (Rpc34)-like	−0.18 ± 0.10	0.21	**−0.93 ± 0.07**	**0.00**	**−1.28 ± 0.18**	**0.01**
At5g46240	Potassium channel protein KAT1	−0.04 ± 0.11	0.49	**−0.93 ± 0.14**	**0.03**	**−1.07 ± 0.19**	**0.01**
At1g01190	Cytochrome P450-like	0.10 ± 0.23	0.26	**−1.99 ± 0.28**	**0.05**	**−2.44 ± 0.30**	**0.00**
At2g46720	Putative β-ketoacyl-CoA synthase	0.15 ± 0.14	0.28	**−1.36 ± 0.21**	**0.03**	**−1.52 ± 0.22**	**0.01**
At1g13080	Putative cytochrome P450 monooxygenase	−0.04 ± 0.12	0.40	**−0.89 ± 0.15**	**0.02**	**−1.09 ± 0.18**	**0.02**
At5g37600	Glutamate–ammonia ligase	−0.31 ± 0.18	0.19	**−1.10 ± 0.16**	**0.02**	**−1.04 ± 0.18**	**0.03**
At3g03000	Putative calmodulin	0.03 ± 0.10	0.39	**−1.06 ± 0.14**	**0.01**	**−1.76 ± 0.50**	**0.02**

Table 5 (*Continued*)

		Control treatments[c,d]		*nhx1* salt-treated[c,e]		Wild-type salt-treated[c,f]	
Accession	Description	Mean ± SE[a]	P[b]	Mean ± SE[a]	P[b]	Mean ± SE[a]	P[b]
At4g11330	MAP kinase (ATMPK5)	0.15 ± 0.17	0.33	**−0.99 ± 0.18**	**0.03**	**−1.19 ± 0.22**	**0.03**
At1g03850	Glutaredoxin-like	−0.33 ± 0.14	0.16	**−3.52 ± 0.46**	**0.00**	**−2.29 ± 0.19**	**0.00**
At1g05320	Myosin-related	0.02 ± 0.12	0.47	**−0.96 ± 0.11**	**0.01**	**−0.93 ± 0.13**	**0.03**
At5g62360	DC1.2 homologue	−0.22 ± 0.15	0.32	**−1.32 ± 0.18**	**0.02**	**−1.11 ± 0.07**	**0.00**
Increased in Atnhx1 control but reduced/restored with salt treatment							
At2g01220	unknown	**1.06 ± 0.15**	**0.01**	**−1.15 ± 0.17**	**0.01**	0.20 ± 0.19	0.35
At4g34830	Putative membrane-associated salt-inducible	**1.57 ± 0.30**	**0.02**	**−1.00 ± 0.15**	**0.02**	0.84 ± 0.33	0.20
At4g14103	Hypothetical	**1.18 ± 0.25**	**0.02**	**−1.91 ± 0.52**	**0.03**	−0.80 ± 0.42	0.21
At4g24290	Expressed	**1.48 ± 0.21**	**0.01**	**−1.38 ± 0.29**	**0.03**	0.23 ± 0.22	0.49
At1g10990	Hypothetical	**1.07 ± 0.24**	**0.03**	**−1.48 ± 0.30**	**0.04**	−1.10 ± 0.37	0.10
At5g67580	Telomere repeat-binding factor 2, myb family (TRB2)	**1.22 ± 0.10**	**0.00**	**−2.54 ± 0.47**	**0.00**	−1.34 ± 0.46	0.09
At1g33470	RNA binding-like	**2.49 ± 0.55**	**0.01**	**−0.98 ± 0.15**	**0.01**	0.87 ± 0.66	0.47
At5g62000	Auxin response factor-like	**1.48 ± 0.22**	**0.02**	**−0.97 ± 0.18**	**0.03**	0.09 ± 0.25	0.42
At2g43160	Putative clathrin-binding protein (epsin)	**1.32 ± 0.24**	**0.02**	**−1.30 ± 0.22**	**0.02**	0.27 ± 0.26	0.42
At1g31680	Putative copper amine oxidase	**1.69 ± 0.36**	**0.02**	**−1.11 ± 0.14**	**0.02**	0.78 ± 0.41	0.29
At5g41180	Receptor kinase-like	**1.04 ± 0.13**	**0.01**	**−1.05 ± 0.16**	**0.02**	0.27 ± 0.19	0.22
At3g17970	Amidase-like	**1.28 ± 0.19**	**0.00**	**−1.16 ± 0.06**	**0.00**	0.68 ± 0.24	0.11
Decreased in Atnhx1 and decreased in wild type because of salt							
At5g15120	Unclassified	**−1.28 ± 0.28**	**0.01**	0.77 ± 0.37	0.19	**−0.90 ± 0.01**	**0.00**
At1g33055	Unclassified	**−1.80 ± 0.17**	**0.00**	0.09 ± 0.30	0.42	**−1.43 ± 0.29**	**0.01**
At3g11745	Unclassified	**−0.96 ± 0.16**	**0.01**	0.10 ± 0.23	0.42	**−0.97 ± 0.17**	**0.02**
At3g62300	Unclassified	**−0.88 ± 0.15**	**0.02**	0.75 ± 0.15	0.03	**−1.30 ± 0.23**	**0.02**
At5g43490	Unclassified	**−0.93 ± 0.13**	**0.01**	0.38 ± 0.19	0.17	**−0.96 ± 0.18**	**0.03**
At1g15270	Unclassified	**−1.03 ± 0.17**	**0.02**	−0.58 ± 0.17	0.07	**−1.04 ± 0.20**	**0.03**
At5g52220	Unclassified	**−1.36 ± 0.19**	**0.02**	0.84 ± 0.22	0.07	**−1.35 ± 0.26**	**0.03**
At4g30330	Small nuclear ribonucleoprotein E homolog	**−0.97 ± 0.18**	**0.03**	−0.43 ± 0.18	0.17	**−1.45 ± 0.23**	**0.01**
At2g28740	Histone H4	**−1.14 ± 0.22**	**0.04**	0.20 ± 0.24	0.49	**−1.33 ± 0.21**	**0.02**
At4g15090	FAR1 family, transposable element	**−0.84 ± 0.12**	**0.01**	0.02 ± 0.16	0.45	**−1.10 ± 0.19**	**0.02**
At1g22590	DNA-binding	**−1.79 ± 0.16**	**0.01**	−0.63 ± 0.16	0.06	**−1.09 ± 0.21**	**0.04**
At3g02340	C3HC4 RING zinc-finger protein	**−0.96 ± 0.17**	**0.03**	−0.18 ± 0.38	0.41	**−1.01 ± 0.18**	**0.05**
At3g48970	GMFP7 isoprenylated homolog	**−1.04 ± 0.22**	**0.03**	0.47 ± 0.26	0.29	**−1.03 ± 0.13**	**0.01**
At4g38420	Putative pectinesterase	**−0.94 ± 0.16**	**0.01**	−0.66 ± 0.41	0.31	**−1.50 ± 0.24**	**0.00**
At3g28740	Cytochrome P450	**−1.20 ± 0.22**	**0.03**	0.04 ± 0.42	0.34	**−2.74 ± 0.32**	**0.01**
At2g36570	Receptor-like protein kinase	**−1.27 ± 0.21**	**0.01**	0.15 ± 0.30	0.41	**−0.93 ± 0.11**	**0.01**
At2g05320	Putative *N*-acetylglucosaminyltransferase	**−0.95 ± 0.14**	**0.01**	0.21 ± 0.28	0.29	**−0.86 ± 0.09**	**0.01**
Decreased in Atnhx1 and further decreased because of salt							
At1g53885	Senescence-associated protein-related	**−1.02 ± 0.16**	**0.04**	**−2.25 ± 0.54**	**0.00**	−0.81 ± 0.32	0.19
Decreased in Atnhx1 and decreased because of salt in both lines							
At5g47240	mutT domain protein-like	**−0.92 ± 0.09**	**0.00**	**−1.18 ± 0.25**	**0.03**	**−1.06 ± 0.06**	**0.00**

[a]Mean numbers represent the log2 transformed ratios (experimental/baseline ± SE) generated when cross-comparing the replicate data sets.
[b]Student's *t*-test *P*-values for data comparison.
[c]Transcript changes that met both statistical criteria for the respective comparison are highlighted in bold.
[d]Comparison of control-treated *nhx1* with control-treated wild-type plant lines.
[e]Comparison of salt-treated *nhx1* with control-treated *nhx1* plant lines.
[f]Comparison of salt-treated wild type with control-treated wild-type plant lines.

stress response remain to be elucidated. One example is KAT1/At5g46240 encoding the guard cell-specific potassium channel KAT1 (Nakamura *et al.*, 1995), and its downregulation would suggest a compromise of guard cell function during salt stress. Only one transcript showed a significantly opposite response to salt stress in the two lines. This transcript (At1g17450) was induced in *nhx1* and reduced in the wild type during salt stress (Tables 3 and 4) and encodes a protein with a weak similarity to the bacterial ATP phosphoribosyltransferase (EC-2.4.2.17). While the role of this protein in plants has not been established, its putative function is the creation of pyrophosphatase using ATP as part of the histidine biosynthesis pathway. A possible contribution to an

increase in the pyrophosphate pool in the *nhx1* knockout plants in response to salt is merely speculative, and while further investigation is needed, the possible contribution of this one exception is intriguing.

Common responses to lack of AtNHX1 and salt stress. The altered expression of 30 genes was similar in knockout plants (grown in the absence of salt) and wild-type plants grown in salt, and only one gene displayed opposite trends (Figure 4, Table 5). These results would indicate similarities between the condition imposed by the absence of AtNHX1 and the stress condition brought about by the salt treatment.

A transcript encoding a peroxidase ATP N (At5g19890) appeared increasingly more upregulated because of salt stress in the *nhx1* line (Table 5). Class III peroxidases play a protective role against stress (Tognolli *et al.*, 2002) and the transcripts show moderate increase in expression with salt stress in the wild type as well. This could indicate a stress condition of the *nhx1* line that was exacerbated by salt. Peroxidases also influence cell size (Andrews *et al.*, 2002) and this protein may be contributing to the reduced cell size of the *nhx1* line (Apse *et al.*, 2003). By contrast, a transcript encoding a protein (At1g53885) that is similar to a senescence-associated protein (SAG102) was reduced in *nhx1* and further reduced by salt. One transcript was significantly affected in all three of the comparisons of this study, encoding an unclassified transcript with a mutT/nudix domain [PF00293] (At5g47240). Similar proteins prevent oxidative-induced mutagenesis (Fowler *et al.*, 2003) and may metabolize nucleoside phosphates as part of the signal transduction processes (Safrany *et al.*, 1998) but its relevance in plants remains to be investigated.

Conclusions

AtNHX1, a vacuolar Na^+/H^+ antiporter of Arabidopsis, plays an important role in ion homeostasis and development, and a T-DNA insertional mutant of *AtNHX1* is compromised in both of these biological characteristics (Apse *et al.*, 2003). We used the T-DNA insertional mutation of *AtNHX1* (*nhx1* plants) and *Affymetrix* ATH1 DNA arrays to assess differences of transcriptional profiles and further characterize the roles of a vacuolar Na^+/H^+ antiporter.

A relatively straightforward approach was used to analyze the DNA microarray data. A combination of cross-wise comparison of replicates and an established method of comparative analysis provided a robust method to determine significance. q-RTPCR analysis asserted the validity of our observations.

Because the plants used in this study were mature, grown in soil and exposed to sub-lethal levels of salt, relatively small changes in gene expression were observed (not many larger than a fourfold response). However, the study of changes in gene expression profiles of soil-grown plants irrigated under control and mild-salt stress regimes provided a good approximation of natural physiological conditions allowing novel insights into the response(s) of Arabidopsis to increased salt concentrations. Interestingly, a larger number of transcripts showed significantly decreased expression (452), rather than increased expression (248), because of salt stress in both the wild-type and *Atnhx1* plant lines. This differs from previous expression studies that did not use soil and/or administered more severe stress (Kawasaki *et al.*, 2001; Kreps *et al.*, 2002; Seki *et al.*, 2002), and emphasizes the significant influence of growth conditions on gene expression.

Notably, there were very few similarities between the gene expression profiles. The comparison of transcription between the *nhx1* and wild-type plants suggests that the AtNHX1 antiporter affects the expression of a variety of plant genes. Furthermore, the absence of functional AtNHX1 appears to significantly alter the profile of salt-responsive transcripts. Moreover, as only a few of the salt-responsive transcripts overlapped with those genes showing induced or reduced expression in the *nhx1* plants, this would imply that most of these latter transcripts did not return to wild-type levels and remained at altered levels.

While there were many notable findings from this study of the Arabidopsis transcriptome, a few stand out as particularly interesting to the role of the AtNHX1 antiporter. Analyses of the transcriptional profile of the AtNHX1 knockout plants growing both in the absence and presence of salt revealed changes in expression of genes encoding proteins associated with intravesicular trafficking (dynamin, clathrin-coated proteins, clathrin-binding proteins, DnaJ, γ SNAP, vacuolar-sorting proteins, etc.), trafficking to the nucleus (karyopherin, importin, etc.), and Golgi processing (*N*-acetylglucosaminyl transferase, UBX) supporting the notion that, similar to the yeast ortholog Nhx1p (Ali *et al.*, 2004), AtNHX1 plays a significant role in protein trafficking and protein targeting, probably via regulation of the acidic intravesicular pH. In addition, relative changes in the expression of NADH dehydrogenase and cytochrome *c* oxidase subunits, together with the downregulation of GUN4 and CRR2 would suggest a link between the altered ion homeostasis (due to the lack of AtNHX1) and the expression and/or assembly of the chloroplast and mitochondrial complexes. Our results suggest that there may also be a link between cellular copper transport/signaling and AtNHX1 function.

Remarkably, very few genes encoding ion transporters were affected in *nhx1* plants. In these plants an increased expression of KUP7/HAK7 was seen, and a reduction in a putative K^+/H^+ antiporter (KEA4) was also observed in the presence of salt. Although the significance of these changes is not clear, these results support the importance of the vacuolar antiporter AtNHX1 in cellular K^+ homeostasis.

It is quite feasible that the changes observed in this study do not reflect the transient effects during other stages of

growth and the stress response (Kreps *et al.*, 2002; Seki *et al.*, 2002). In order to clarify the role of AtNHX1 during the early stages of stress (osmotic and ion balance) and growth (cell division, cell expansion, source/sink transitions, etc.) transcriptome analyses at shorter time intervals of salt stress are needed. These experiments are now in progress.

Experimental procedures

Plant material

Two lines of *A. thaliana* ecotype Wassilewskija were used for this study, wild-type line (WS) and a *nhx1* 'knockout' line with a T-DNA insertion in the ninth exon of the *AtNHX1* gene (Apse *et al.*, 2003). The plants were grown for a total of 30 days prior to RNA extraction. The growth period was initiated by the germination of bleach-sterilized seeds on 8% agar plates containing 5% sucrose and a modified MS growth medium used by Apse *et al.* (2003). Seedlings were grown under a 12-h photoperiod at 22°C in a growth chamber (Model CU-36L; Percival Scientific, Perry, IA, USA). Seeds were plated in Petri dishes at an even density of approximately 1 seed cm^{-2}. After 2 weeks of growth, the seedlings were transferred to moist soil (MetroMix 200; Scotts Sierra Horticulture Products, Marysville, OH, USA). Seedlings (five per pot) were grown on 100 ml pots (Kord Products, Bramalea, Ont., Canada). The pots were covered with a transparent plastic cover and grown in a growth chamber (Model AC-40 Controller 6000; Enconair, Winnipeg, MB, Canada) at 22°C under a short-day cycle (8 h light, 16 h dark) in order to increase the leaf area and growth of seedlings while not promoting bolting. Following a 2-day acclimation period, plants were watered to soil saturation using the growth medium described above, without sucrose. Watering was repeated every 3–4 days. A week before harvest inflorescence tissues were removed to further emphasize leaf growth and to help minimize developmental differences among plants. At harvest, all plant tissue, except for roots and inflorescences, was immediately frozen under liquid nitrogen. Plants subjected to salt stress were watered for 2 weeks with growth medium supplemented with 100 mM NaCl. Independent biological samples were harvested and subsets (22–25 plants) were pooled and selected for subsequent analysis. Four samples for control treatments and three salt-stressed samples of both the WS and the AtNHX1 lines were selected.

RNA extraction and GeneChip® hybridization

Each pool of tissue for RNA extraction consisted of material from 22–25 plants (approximately 3 g of fresh tissue). Frozen tissue was ground to powder using an RNase-free mortar and pestle and RNA was extracted by a modification of the hot-phenol method (Verwoerd *et al.*, 1989). After quality confirmation by agarose gel analysis and RT-PCR, the extracted RNA was prepared for array analysis as described by the manufacturer (*Affymetrix® GeneChip® Expression Analysis Technical Manual*; http://www.affymetrix.com), using the chemicals and reagents suggested. Briefly, ds-cDNA was made from total RNA, followed by formation of biotin-labeled cRNA, which was purified and fractionated prior to hybridization on individual gene chips. After overnight hybridization, the chips were stained with streptavidin–phycoerythrin and biotinylated anti-streptavidin antibody, then scanned by laser, producing a data image software file, the basis for quantifying and comparing relative transcript levels. Quantification of the data files depends on a number of mathematical factors as optimized by Affymetrix® (http://www.affymetrix.com/support/technical/technotes/statistical_algorithms_technote.pdf) but is primarily based on the hybridization of experimental RNA to 11 sets of representative 25-mer probes on the chip, each set consisting of both a perfect match and a single mismatch oligomer sequence complementing unique portions of different transcripts. For this study, the *Affymetrix®* ATH1-121501 Genome Array *GeneChip®* was used, containing probe sets for 22 746 predicted and known expressed Arabidopsis genes.

Data analysis

Data images produced after microarray scanning were interpreted by Affymetrix® Microarray Suite 5.0 (MAS 5.0) software with scaling of all probe sets to a target value of 500. The purpose of this chip-wide scaling was to minimize chip-to-chip difference in overall hybridization intensities (http://www.affymetrix.com/Auth/support/downloads/manuals/data_analysis_fundamentals_manual.pdf). A text file of all the data was produced and any transcript that did not generate a detection *P*-value <0.05 (http://www.affymetrix.com/support/technical/technotes/statistical_reference_guide.pdf) for at least three chips was removed from the analysis (the default *P*-value cut-off for a 'present' expression call is 0.065). This left 13 144 genes for further analysis. This filter eliminated 9602 genes with unreliable expression data; that was either too low to be considered significantly 'present' or had match/mismatch ratios that were too high to rule out non-specific binding of the probes. This also eliminated the large majority of transcripts with non-normal distribution of detection value data generated by MAS 5.0 algorithms (Giles and Kipling, 2003). Data from the remaining 13 144 genes were first normalized to an invariant set using dChip v1.2 computer software (http://www.dchip.org/; Li and Wong, 2001) before export into Microsoft® Excel® (Microsoft Corp., Redmond, WA, USA) as separate data sets for each chip in spreadsheet form.

A cross-wise $\log_2$ ratio analysis was performed using the data generated after invariant set normalization. The raw numerical numbers for each replicate of the experimental data were divided by each replicate of the baseline data. For example, with three replicates of a treated sample and four replicates of the untreated sample, 12 different comparisons were generated (Figure 5). These comparisons were log-transformed (base 2) and averaged. As a cut-off, the average log ratio of a comparison needed to be more than two standard errors from a log change ratio of 0.585. This value corresponds to a 95% degree of certainty that the true mean represents at least a 50% deviation from the baseline control. To add further to the certainty of the differences between the experimental setups, one-tailed Student's *t*-tests (homoscedastic) were used to evaluate the statistical significance of the difference of expression data values used for comparisons. A cut-off of $P < 0.05$ was used, signifying 95% certainty that the two sets of values compared were from different populations and therefore distinct. Transcripts with detection levels that met both these criteria were regarded as *significantly* altered in expression and are emphasized for this study. (Data for the gene transcripts that meet either of the criteria sets can be found at http://blumwald.ucdavis.edu/microarrays.)

Functional classification

In order to classify genes of interest with significant changes in expression level detection, the MIPS MATDB web database (http://mips.gsf.de/proj/thal/db/index.html) was consulted. The TIGR (http://www.tigr.org/tdb/e2k1/ath1/index.shtml) and TAIR (http://www.arabidopsis.org) web databases were also used for

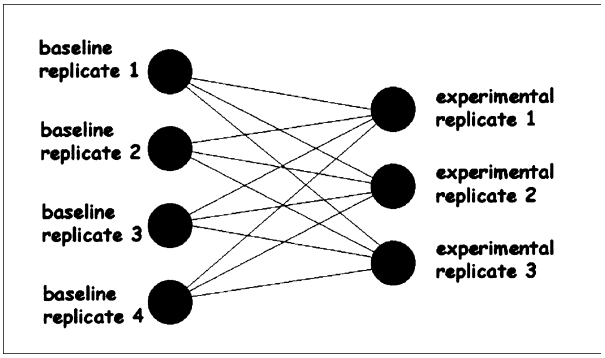

Figure 5. Cross-wise experimental comparison.

less certain classifications. Genes were classified according to their most likely role, and an assignment of 'unclassified' was given in those cases where either a predicted function or similarity with other known genes of known function was not apparent. All classifications are based on information available at the time of analysis, and may have since been revised or updated.

Functional classifications are based on the following criteria: *Unclassified*: no putative function or similarity to other genes were determined. *Transcription*: genes encoding putative DNA-binding proteins – such as transcription factors, DNA repair proteins, and mRNA-processing proteins – but not including genes encoding proteins likely involved with cell cycle/DNA synthesis. *Transport/ion homeostasis*: genes encoding transporters (ion, sugar, amino acid, etc.) and ion-binding proteins, excluding those genes encoding proteins likely involved in energy-related transport and Signaling. *Metabolism*: includes genes encoding for proteins that are putatively involved in metabolic processes such as biosynthesis and other enzymatic reactions but not including energy-related enzymes or structure-related metabolites. *Translation*: includes genes encoding proteins associated with ribosomal complexes and other key enzymes involved in protein synthesis. *Signaling*: genes encoding those proteins involved in signal transduction and perception such as kinases, phosphatases, and calcium-binding proteins. *Energy transduction*: includes genes encoding proteins involved in energy transduction within the plant such as those associated with photosynthesis, respiration, and general redox reactions. Also includes genes encoded by either the chloroplast or mitochondria genomes. *Processing*: genes encoding proteins involved in the modification, transport, and/or degradation of proteins; for example; vesicular trafficking proteins, chaperones, and proteases. *Growth/structure*: genes encoding proteins with the primary function of regulating and promoting cell division and genes encoding proteins that make up the cell structure, including cytoskeletal elements and cell wall components. *Defense*: includes genes encoding proteins most closely associated with the plant response to disease.

Protein families and domains are referenced by the Sanger Institute Pfam database (http://www.sanger.ac.uk/Software/Pfam/) and are annotated as [PFXXXXX] where appropriate.

Quantitative reverse transcriptase PCR

cDNA was synthesized using the iScript™ cDNA Synthesis Kit (Bio-Rad Laboratories, Hercules, CA, USA) under the conditions suggested by the manufacturer using as starting material the same RNA samples that were used for microarray analysis. Real-time PCR was subsequently performed with the iQ™ SYBR® Green Supermix (Bio-Rad Laboratories) according to guidelines specified by the manufacturer. For signal detection, the iCycler Optical System (Bio-Rad Laboratories) was used. Four or more standards using different known dilutions were run with every reaction for quantification purposes. Eighteen genes with at least one significant sample difference based on microarray data were selected for q-RTPCR analysis, along with a single gene that did not (At4g39350). Three or more independent qRT-PCR replicates of the 18 selected genes were performed with each sample type (wild type, salt-stressed wild type, *nhx1*, salt-stressed *nhx1*) and run simultaneously. Data for each replicate set were scaled as needed to adjust for standardization discrepancies. Log_2 ratios for each replicate and their averages and standard errors were calculated. Primers were designed based on the probe sequences used by Affymetrix® with a target size range between 280 and 320 base pairs (Table S1).

Acknowledgements

This research was supported by grants from the National Science Foundation (IBN-0110622) and Arcadia BioSciences Inc. We thank Toshio Yamaguchi for helpful discussions.

Supplementary Material

The following material is available from http://www.blackwellpublishing.com/products/journals/suppmat/TPJ/TPJ2253/TPJ2253sm.htm.

Table S1 Transcripts displaying increased expression in the *nhx* 1 line

Table S2 Transcripts displaying decreased expression in the *nhx* 1 line

Table S3 Transcripts with significantly increased expression as a result of salt treatment

Table S4 Transcripts with significantly decreased expression as a result of salt treatment

Table S5 Transcripts and primers used for quantitative RT-PCR verification

References

Aharon, G.S., Apse, M.P., Duan, S., Hua, X. and Blumwald, E. (2003) Characterization of a family of vacuolar Na^+/H^+ antiporters in *Arabidopsis thaliana*. *Plant Soil*, **253**, 245–256.

Ahmed, S.U., Rojo, E., Kovaleva, V., Venkataraman, S., Dombrowski, J.E., Matsuoka, K. and Raikhel, N.V. (2000) The plant vacuolar sorting receptor AtELP is involved in transport of NH2-terminal propeptide-containing vacuolar proteins in *Arabidopsis thaliana*. *J. Cell Biol.* **149**, 1335–1344.

Ahn, S.J., Shin, R. and Schachtman, D.P. (2004) Expression of *KT/KUP* genes in Arabidopsis and the role of root hairs in K^+ uptake. *Plant Physiol.* **134**, 1135–1145.

Ali, R., Brett, C.L., Mukherjee, S. and Rao, R. (2004) Inhibition of sodium/proton exchange by a Rab-GTPase-activating protein regulates endosomal traffic in yeast. *J. Biol. Chem.* **279**, 4498–4506.

Andrews, J., Adams, S.R., Burton, K.S. and Edmondson, R.N. (2002) Partial purification of the tomato fruit peroxidase and its effect on the mechanical properties of tomato fruit skin. *J. Exp. Bot.* **53**, 2393–2399.

Apse, M.P., Aharon, G.S., Snedden, W.A. and Blumwald, E. (1999) Salt tolerance conferred by overexpression of a vacuolar Na+/H+ antiport in *Arabidopsis*. *Science*, **285**, 1256–1258.

Apse, M.P., Sottosanto, J.B. and Blumwald, E. (2003) Vacuolar cation/H^+ exchange, ion homeostasis, and leaf development are altered in a T-DNA insertional mutant of *AtNHX1*, the *Arabidopsis* vacuolar Na^+/H^+ antiporter. *Plant J.* **36**, 229–239.

Arondel, V., Vergnolle, C., Cantrel, C. and Kader, J.C. (2000) Lipid transfer proteins are encoded by a small multigene family in *Arabidopsis thaliana*. *Plant Sci.* **157**, 1–12.

Aukerman, M.J., Lee, I., Weigel, D. and Amasino, R.M. (1999) The Arabidopsis flowering-time gene *LUMINIDEPENDENS* is expressed primarily in regions of cell proliferation and encodes a nuclear protein that regulates *LEAFY* expression. *Plant J.* **19**, 195–203.

Balmer, Y., Vensel, W.H., Tanaka, C.K. *et al.* (2004) Thioredoxin links redox to the regulation of fundamental processes of plant mitochondria. *Proc. Natl Acad. Sci. USA*, **101**, 2642–2647.

Blumwald, E. (1987) Tonoplast vesicles as a tool in the study of ion-transport at the plant vacuole. *Physiol. Plant.* **69**, 731–734.

Bowers, K., Levi, B.P., Patel, F.I. and Stevens, T.H. (2000) The sodium/proton exchanger Nhx1p is required for endosomal protein trafficking in the yeast *Saccharomyces cerevisiae*. *Mol. Biol. Cell*, **11**, 4277–4294.

Cho, H.T. and Cosgrove, D.J. (2000) Altered expression of expansin modulates leaf growth and pedicel abscission in *Arabidopsis thaliana*. *Proc. Natl Acad. Sci. USA*, **97**, 9783–9788.

Curi, G.C., Welchen, E., Chan, R.L. and Gonzalez, D.H. (2003) Nuclear and mitochondrial genes encoding cytochrome *c* oxidase subunits respond differently to the same metabolic factors. *Plant Physiol. Biochem.* **41**, 689–693.

Espartero, J., Sanchez-Aguayo, I. and Pardo, J.M. (1995) Molecular characterization of glyoxalase-I from a higher plant; upregulation by stress. *Plant Mol. Biol.* **29**, 1223–1233.

Eulgem, T., Rushton, P.J., Robatzek, S. and Somssich, I.E. (2000) The WRKY superfamily of plant transcription factors. *Trends Plant Sci.* **5**, 199–206.

Fowler, R.G., White, S.J., Koyama, C., Moore, S.C., Dunn, R.L. and Schaaper, R.M. (2003) Interactions among the *Escherichia coli mutT, mutM*, and *mutY* damage prevention pathways. *DNA Repair*, **2**, 159–173.

Giles, P.J. and Kipling, D. (2003) Normality of oligonucleotide microarray data and the implications for parametric statistical analyses. *Bioinformatics*, **19**, 2254–2262.

Haecker, A., Gross-Hardt, R., Geiges, B., Sarkar, A., Breuninger, H., Herrmann, M. and Laux, T. (2004) Expression dynamics of WOX genes mark cell fate decisions during early embryonic patterning in *Arabidopsis thaliana*. *Development*, **131**, 657–668.

Hashimoto, M., Endo, T., Peltier, G., Tasaka, M. and Shikanai, T. (2003) A nucleus-encoded factor, CRR2, is essential for the expression of chloroplast ndhB in Arabidopsis. *Plant J.* **36**, 541–549.

Hernandez, J.A., Jimenez, A., Mullineaux, P. and Sevilla, F. (2000) Tolerance of pea (Pisum sativum L.) to long-term salt stress is associated with induction of antioxidant defences. *Plant Cell Environ.* **23**, 853–862.

Jung, H.W., Kim, W. and Hwang, B.K. (2003) Three pathogen-inducible genes encoding lipid transfer proteins from pepper are differently activated by pathogens, abiotic, and environmental stresses. *Plant Cell Environ.* **26**, 915–928.

Kawasaki, S., Borchert, C., Deyholos, M., Wang, H., Brazille, S., Kawai, K., Galbraith, D. and Bohnert, H.J. (2001) Gene expression profiles during the initial phase of salt stress in rice. *Plant Cell*, **13**, 889–905.

Klien, D. (2002) Quantification using real-time PCR technology: applications and limitations. *Trends Mol. Med.* **8**, 257–260.

Kreps, J.A., Wu, Y.J., Chang, H.S., Zhu, T., Wang, X. and Harper, J.F. (2002) Transcriptome changes for Arabidopsis in response to salt, osmotic, and cold stress. *Plant Physiol.* **130**, 2129–2141.

Larkin, R.M., Alonso, J.M., Ecker, J.R. and Chory, J. (2003) GUN4, a regulator of chlorophyll synthesis and intracellular signaling. *Science*, **299**, 902–906.

Lee, M.-L.T., Kuo, F.C., Whitmore, G.A. and Sklar, J. (2000) Importance of replication in microarray gene expression studies: statistical methods and evidence from repetitive cDNA hybridizations. *Proc. Natl Acad. Sci. USA*, **97**, 9834–9839.

Lenhard, M., Jurgens, G. and Laux, T. (2002) The WUSCHEL and SHOOTMERISTEMLESS genes fulfill complementary roles in Arabidopsis shoot meristem regulation. *Development*, **129**, 3195–3206.

Li, C. and Wong, W.H. (2001) Model-based analysis of oligonucleotide arrays: expression index computation and outlier detection. *Proc. Natl Acad. Sci. USA*, **98**, 31–36.

Li, Y., Jones, L. and McQueen-Mason, S. (2003) Expansins and cell growth. *Curr. Opin. Plant Biol.* **6**, 603–610.

Lin, Y., Sun, L., Nguyen, L.V., Rachubinski, R.A. and Goodman, H.M. (1999) The pex16p homolog *SSE1* and storage organelle formation in Arabidopsis seeds. *Science*, **284**, 328–330.

Lu, C. and Vonshak, A. (2002) Effects of salinity stress on photosystem II function in cyanobacterial *Spirulina platensis* cells. *Physiol. Plant.* **114**, 405–413.

Maathuis, F.J.M., Filatov, V., Herzyk, P. *et al.* (2003) Transcriptome analysis of root transporters reveals participation of multiple gene families in the response to cation stress. *Plant J.* **35**, 675–692.

Mäser, P., Thomine, S., Schroeder, J.I. *et al.* (2001) Phylogenetic relationships within cation transporter families of Arabidopsis. *Plant Physiol.* **126**, 1646–1667.

Milla, M.A.R., Maurer, A., Huete, A.R. and Gustafson, J.P. (2003) Glutathione peroxidase genes in *Arabidopsis* are ubiquitous and regulated by abiotic stresses through diverse signaling pathways. *Plant J.* **36**, 602–615.

Mittova, V., Tal, M., Volokita, M. and Guy, M. (2002) Salt stress induces up-regulation of an efficient chloroplast antioxidant system in the salt-tolerant wild tomato species *Lycopersicon pennellii* but not in the cultivated species. *Physiol. Plant.* **115**, 393–400.

Nakagawa, Y. and Imai, H. (2000) Novel functions of mitochondrial phospholipids hydroperoxide glutathione peroxidase (PHGPx) as an anti-apoptotic factor. *J. Health Sci.* **46**, 414–417.

Nakamura, R.L., McKendree, W.L., Hirsch, R.E., Sedbrook, J.C., Gaber, R.F. and Sussman, M.R. (1995) Expression of an Arabidopsis potassium channel gene in guard cells. *Plant Physiol.* **109**, 371–374.

Narayan, S., Jaiswal, A.S., Multan, A.S. and Pathak, S. (2001) DNA damage-induced cell cycle checkpoints involve both p53-dependent and -independent pathways: role of telomere repeat binding factor 2. *Br. J. Cancer*, **85**, 898–901.

Noctor, G., Gomez, L., Vanacker, H. and Foyer, C.H. (2002) Interactions between biosynthesis, compartmentation and transport in the control of glutathione homeostasis and signalling. *J. Exp. Bot.* **53**, 1283–1304.

Pan, W., Lin, J. and Le, C.T. (2002) How many replicates of arrays are required to detect gene expression changes in microarray experiments? A mixture model approach. *Genome Biol.* **3**, 1–10.

Quiles, M.J. and Lopez, N.I. (2004) Photoinhibition of photosystems I and II induced by exposure to high light intensity during oat plant growth – effects on the chloroplast NADH dehydrogenase complex. *Plant Sci.* **166**, 815–823.

Rees, E.M. and Thiele, D.J. (2004) From aging to virulence: forging connections through the study of copper homeostasis in eukaryotic microorganisms. *Curr. Opin. Microbiol.* **7**, 175–184.

Safrany, S.T., Caffrey, J.J., Yang, X., Bembenek, M.E., Moyer, M.B., Burkhart, W.A. and Shears, S.B. (1998) A novel context for the 'MutT' module, a guardian of cell integrity, in a diphosphoinositol polyphosphate phosphohydrolase. *EMBO J.* **17**, 6599–6607.

Sedbrook, J.C., Chen, R.J. and Masson, P.H. (1999) ARG1 (Altered Response to Gravity) encodes a DnaJ-like protein that potentially interacts with the cytoskeleton. *Proc. Natl Acad. Sci. USA*, **96**, 1140–1145.

Seki, M., Narusaka, M., Ishida, J. *et al.* (2002) Monitoring the expression profiles of 7000 Arabidopsis genes under drought, cold and high-salinity stresses using a full-length cDNA microarray. *Plant J.* **31**, 279–292.

Senn, M.E., Rubio, F., Banuelos, M.A. and Rodriguez-Navarro, A. (2001) Comparative functional features of plant potassium HvHAK1 and HvHAK2 transporters. *J. Biol. Chem.* **276**, 44563–44569.

Shi, H. and Zhu, J.-K. (2002) Regulation of the vacuolar Na^+/H^+ antiporter gene *AtNHX1* expression by salt stress and ABA. *Plant Mol. Biol.* **50**, 543–550.

Shi, H., Ishitani, M., Kim, C.S. and Zhu, J.-K. (2000) The *Arabidopsis thaliana* salt tolerance gene SOS1 encodes a putative Na^+/H^+ antiporter. *Proc. Natl Acad. Sci. USA*, **97**, 6896–6901.

Singla-Pareek, S.L., Reddy, M.K. and Sopory, S.K. (2003) Genetic engineering of the glyoxalase pathway in tobacco leads to enhanced salinity tolerance. *Proc. Natl Acad. Sci. USA*, **100**, 14672–14677.

Stenbeck, G. (1998) Soluble NSF-attachment proteins. *Int. J. Biochem. Cell Biol.* **30**, 573–577.

Su, H., Golldack, D., Zhao, C. and Bohnert, H.J. (2002) The expression of HAK-type K^+ transporters is regulated in response to salinity stress in common ice plant. *Plant Physiol.* **129**, 1482–1493.

Szczypka, M.S., Zhu, Z., Silar, P. and Thiele, D.J. (1997) *Saccharomyces cerevisiae* mutants altered in vacuole function are defective in copper detoxification and iron-responsive gene transcription. *Yeast*, **13**, 1432–1435.

Taji, T., Seki, M., Yamaguchi-Shinozaki, K., Kamada, H., Giraudat, J. and Shinozaki, K. (1999) Mapping of 25 drought-inducible genes, RD and ERD, in *Arabidopsis thaliana*. *Plant Cell Physiol.* **40**, 119–123.

Takahashi, S., Katagiri, T., Yamaguchi-Shinozaki, K. and Shinozaki, K. (2000) An *Arabidopsis* gene encoding a Ca^{2+}-binding protein is induced by abscisic acid during dehydration. *Plant Cell Physiol.* **41**, 898–903.

Tognolli, M., Penel, C., Greppin, H. and Simon, P. (2002) Analysis and expression of the class III peroxidase large gene family in *Arabidopsis thaliana*. *Gene*, **288**, 129–138.

Venema, K., Quintero, F.J., Pardo, J.M. and Donaire, J.P. (2002) The *Arabidopsis* Na^+/H^+ exchanger AtNHX1 catalyzes low affinity Na^+ and K^+ transport in reconstituted liposomes. *J. Biol. Chem.* **277**, 2413–2418.

Verwoerd, T.C., Dekker, B.M. and Hoekema, A. (1989) A small-scale procedure for the rapid isolation of plant RNAs. *Nucleic Acids Res.* **17**, 2362.

Yamaguchi, T., Fukada-Tanaka, S., Inagaki, Y., Saito, N., Yonekura-Sakakibara, K., Tanaka, Y., Kusumi, T. and Iida, S. (2001) Genes encoding the vacuolar Na^+/H^+ exchanger and flower coloration. *Plant Cell Physiol.* **42**, 451–461.

Yamamoto, Y.Y., Deng, X.W. and Matsui, M. (2001) ClP4, a new COP1 target, is a nucleus-localized positive regulator of Arabidopsis photomorphogenesis. *Plant Cell*, **13**, 399–411.

Yokoi, S., Quintero, F.J., Cubero, B., Ruiz, M.T., Bressan, R.A., Hasegawa, P.M. and Pardo, J.M. (2002) Differential expression and function of *Arabidopsis thaliana* NHX Na^+/H^+ antiporters in the salt stress response. *Plant J.* **30**, 529–539.

Yoshiba, Y., Aoki, C., Iuchi, S., Nanjo, T., Seki, M., Sekiguchi, F., Yamaguchi-Shinozaki, K. and Shinozaki, K. (2001) Characterization of four extensin genes in *Arabidopsis thaliana* by differential gene expression under stress and non-stress conditions. *DNA Res.* **8**, 115–122.

Zhang, H.X. and Blumwald, E. (2001) Transgenic salt-tolerant tomato plants accumulate salt in foliage but not in fruit. *Nat. Biotechnol.* **19**, 765–768.

Zhang, H.X., Hodson, J.N., Williams, J.P. and Blumwald, E. (2001) Engineering salt-tolerant *Brassica* plants: characterization of yield and seed oil quality in transgenic plants with increased vacuolar sodium accumulation. *Proc. Natl Acad. Sci. USA*, **98**, 12832–12836.